RESEARCH DEPARTMENT REPORT SERIES no. 26/2007 ISSN 1749-8775

AN INVESTIGATION OF HAMMERSCALE

TECHNOLOGY REPORT

David Dungworth and Roger Wilkes

ARCHAEOLOGICAL SCIENCE

ENGLISH HERITAGE

Research Department Report 26/2007

An investigation of hammerscale

D Dungworth and R Wilkes

ISSN 1749-8775

The Research Department Report Series, incorporates reports from all the specialist teams within the English Heritage Research Department: Archaeological Science; Archaeological Archives; Historic Interiors Research and Conservation; Archaeological Projects; Aerial Survey and Investigation; Archaeological Survey and Investigation; Architectural Investigation; Imaging, Graphics and survey, and the Survey of London. It replaces the former centre for Archaeology Report Series, the Archaeological Investigation Series, and the Architectural Investigation Report Series.

Many of these reports are interim reports which make available the results of specialist investigations in advance of full publication. They are not subject to external refereeing, and their conclusions may sometimes have to be modified in the light of archaeological information that was not available at the time of the investigation. Where no final project report is available, readers are advised to consult the author before citing these reports in any publication. Opinions expressed in Research Department reports are those of the author(s) and are not necessarily those of English Heritage.

Research Department Report 26/2007

An investigation of hammerscale

D Dungworth and R Wilkes

Summary

Archaeologists regularly recover hammerscale from archaeological deposits. This material is particularly useful as it indicates the hot-working or iron and iron alloys. Hammerscale is commonly found as small flakes which are comparable to the scale produced in modern steel works during the hot working of iron and its alloys. Less common are small spheres but these are usually found with flake hammerscale, and like the flake hammerscale they are magnetic. This project has examined flake and spheroid hammerscale from archaeological contexts and undertaken forging and fire-welding experiments to test the hypothesis that spheres are produced during fire-welding. Several lines of enquiry indicate that the spheres are produced by traditional fire-welding; a phenomenon which was most clearly illustrated by the high-speed digital video of an experimental weld. The SEM-EDS examination of the archaeological and experimental hammerscale suggests that the non-metallic (slag) inclusions in the metal make a significant contribution to the formation of hammerscale.

Keywords

Metal Working Fe

Author's address

English Heritage, Fort Cumberland, Fort Cumberland Road, Eastney, Portsmouth, PO4 9LD.
Telephone: 02392 856783. Email: david.dungworth@english-heritage.org.uk
Telephone: 02392 856784. Email: roger.wilkes@english-heritage.org.uk

Contents

The CD in the wallet at the back of this report contains an electronic Adobe Acrobat version of this report and two digital movies:

lowspeed.avi	shows an extract from the conventional (25fps) video Figure 11 of this report was captured from this video
highspeed.avi	shows an extract from the high-speed (600fps) video Figures 13–17 of this report were captured from this video

Introduction

This report provides results of the scientific examination of samples of hammerscale from archaeological excavations and from replication experiments. The primary aim was to establish the circumstances under which spheroidal hammerscale formed. This introduction describes the background and scope of the project and defines some of the terms used. The two following sections describe the history of the study of hammerscale and the methods used in this project. The next three sections detail the examination of samples of hammerscale recovered from two archaeological excavations and from the replication experiments. The results are discussed and models for the formation of hammerscale are set out.

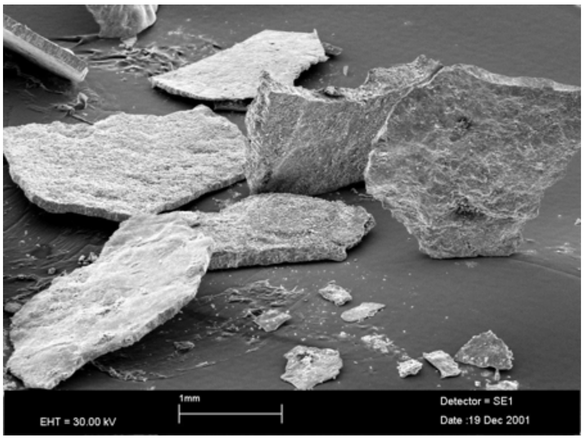

Figure 1. Flake hammerscale

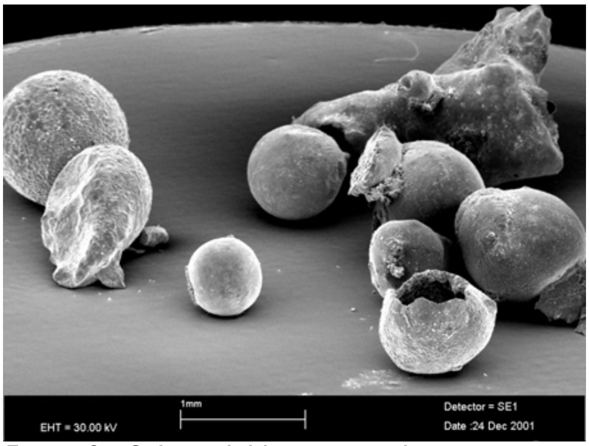

Figure 2. Spheroidal hammerscale

Hammerscale is a shiny, black, magnetic waste product which forms during the hot working of iron and its alloys. It is usually in the form of small plates, sheets or flakes several millimetres across and less than a millimetre thick (Figure 1). In modern industrial contexts the material is frequently encountered as a waste product during the hot rolling of steel and is usually referred to as mill-scale (Garber 1959). Hammerscale has been recognised in archaeological contexts for over 60 years (see below). Archaeological samples of hammerscale usually contain a morphologically distinct form of hammerscale: tiny spheroids (Figure 2). These spheroids have been subjected to limited scientific research and, while it has become widely accepted that they are a waste product from fire-welding, there has been no proof of this.

This project was undertaken to improve knowledge of hammerscale from archaeological contexts and in particular to determine whether or not spheroidal hammerscale was produced by welding. To achieve this aim, samples of hammerscale (both flake and spheroid) from two archaeological sites were selected for study. A series of simple experiments were undertaken to replicate forging and fire-welding of iron and steel in order to recover the hammerscale produced in each case. In addition, a high-speed digital video camera was used to record several fire-welds.

For the purposes of this report, we regard iron working as a blanket term which covers all iron smelting and smithing activities. Iron smithing is used where we wish to exclude smelting activities. Iron forging is used to describe the hot-working or smithing of iron without the use of welding. Fire-welding is used to denote traditional welding techniques, ie those which use just heat and the force of a hammer blow.

Previous Studies of Hammerscale

Early 20th-century archaeological excavation of blacksmiths' workshops (eg Forster and Knowles 1910; 1913) often refer to the presence of smithing hearths as well as scrap metal and part-made objects. Less frequently these early reports describe the occupation horizon within these workshops as black. With hindsight we can suggest that these layers were probably rich in hammerscale; however, the modes of excavation and recording then used did not allow its recognition.

The earliest explicit recognition of hammerscale in the archaeological literature of England comes from the 1941 report of an excavation of the Roman fort of Benwell on Hadrian's Wall (Simpson and Richmond 1941). The excavators were intrigued by the presence of a black layer and sent samples of this to Smythe who carried out chemical analysis that showed,

> In the main, the material is the magnetic oxide of iron Fe_3O_4, containing ferrous oxide in considerable amount and some metallic iron. There can be no doubt that it is a mill-scale or smithy scale, and that the deposit is derived from the sweepings of a black smiths shop
> Smythe in Simpson and Richmond 1941, 41

The excavation of a Roman iron smelting site at Ashwicken, Norfolk (Tylecote and Owles 1960) revealed large deposits of hammerscale. The examination with an optical microscope of a cross-section through a sample of hammerscale showed that it 'contained 85.8 per cent of magnetite, the remainder being cementing films of fayalite' (ibid, 149, fig 9). Tylecote (1962, 254) describes hammerscale as forming during the heating and forging of iron and suggests that several different oxides of iron may be formed, including ferrous iron oxide (FeO), magnetite (Fe_3O_4) and ferric oxide (Fe_2O_3). He also proposes that most of the silica in the cementing films derives from the slag inclusions in the iron and possibly from the use of sand as a flux (ibid, 255).

McDonnell (1984) identified two types of hammerscale on the basis of their shapes: flakes and hollow spheroids. He observed that flakes of hammerscale were much more abundant than spheroids. Cross-sections of both types of hammerscale were examined with a scanning electron microscope and the chemical compositions determined using an energy dispersive X-ray analyser. He concluded that both types had similar microstructures but that the spheroids, which were often hollow, contained greater amounts of phosphorus. Subsequently he suggested that the spheroids were produced during the fire-welding of iron and that a sand flux was important in their formation (McDonnell 1986). He proposed that the oxidised surface of the iron and the sand flux would react together. When two pieces of metal were welded together, the heat and the pressure combined to extrude this slag which would then be 'cooled in flight' (ibid, 146). Later he also suggested that hammerscale was an important source of material for the formation of smithing slags (McDonnell 1991).

Mills and McDonnell (1992) carried out an intensive programme of hammerscale recovery from a medieval blacksmithy at Burton Dassett. This included the collection of hundreds of soils samples arranged on a grid throughout the building. The proportion of hammerscale in each sample was plotted to reveal spatial concentrations (and lacunae) which indicated the locations of the smithing hearth and the anvil block (neither of these features survived to be recognised by any other means).

Allen (1986) described in detail the morphology of hammerscale and related debris recovered from an eroding section on the edge of the river Severn. The material probably derived from a Roman period workshop where blooms were consolidated into bars. Allen identified twelve different types of hammerscale on the basis of their size and shape but it is clear than flakes were the most common type and the others made up a very small proportion of the assemblage. Allen's detailed typology for hammerscale has not been widely adopted.

Unglik (1991) examined a large quantity of hammerscale from an early 19th-century blacksmithy in Canada. This assemblage included both flakes and spheroids: the former averaged 0.3mm in thickness while the latter averaged 2mm in diameter, with 66% of them being hollow. Samples of each were mounted in cross-section for an examination of their microstructures. Both types of hammerscale were found to be composed of magnetite and wüstite crystals, with a fayalite bonding. Unglik found that some of the spheroids had highly dendritic iron oxide (implying a rapid cooling rate) while the flakes often had a 'featureless oxide scale structure' (1991, 96).

Sim (1998) examined Roman hammerscale from Silchester and produced hammerscale during the experimental replication of many iron smithing activities. The experiments demonstrated that most hammerscale consists of flakes and that these were deposited close to the anvil. The examination of the experimentally produced hammerscale showed that small quantities of spheroidal hammerscale were produced during welding. Limited chemical analyses were undertaken which revealed that all samples were rich in iron oxide and silica but that the iron oxide to silica ratio varied depending on the metal being worked. Well-refined billets gave hammerscale with high iron oxide content while less well-refined iron gave hammerscale richer in silica.

The examination by Paynter (2002) of smelting and smithing debris from the Roman settlement at Westhawk Farm included several samples of hammerscale. Sections through smithing slags revealed the presence of fragments of hammerscale and confirmed McDonnell's (1991) suggestion that hammerscale was an important 'ingredient' in smithing slags.

Hammerscale is now routinely recovered from archaeological soil samples (Bayley *et al* 2001). Flake hammerscale is the most abundant form and there is no doubt that it forms due to the partial oxidation of the surface of iron as it is heated in a hearth prior to smithing. When the hot iron is struck with a hammer, the relatively soft iron plastically deforms while the brittle scale on the surface flakes off and is deposited around the anvil. Spheroidal hammerscale has been recognised from archaeological contexts for several decades but its origins are less well understood. It is widely accepted that spheroids, which are often hollow, were molten and have cooled rapidly. The most popular model for its formation is fire-welding. It is assumed that the combination of temperature and pressure is enough to first melt the two layers of scale present in a weld and then eject it as a liquid which forms spheroids as it travels through the air. None of the previous work outlined above, however, provides any proof that this model is correct. The remainder of this report describes the examination of archaeological samples of hammerscale and replication experiments undertaken in an attempt to verify this model.

Laboratory Methods

Samples of hammerscale were obtained from archaeological sites and from replication experiments. The samples from archaeological sites derived from soil samples taken from dark 'occupation soils' within workshops used for smithing iron objects. The archaeological soil samples were sieved to remove clay- and silt-sized particles and the magnetic fraction separated with a magnet. The samples from the replication experiments were collected using a dustpan and brush. Examination of the dried magnetic residues showed the presence of flake and spheroidal hammerscale. Samples were selected and photographed using a digital camera with low power microscope (up to 40 time magnification) and using a scanning electron microscope (SEM: Carl Zeiss S440i, secondary electron detector). The samples were then mounted in epoxy resin mounted, and ground and polished to reveal a cross-section. These samples were examined using the SEM in back scatter mode and the chemical composition determined using an energy dispersive X-ray detector (Oxford Instruments germanium detector; deconvolution and quantification by ISIS SEMQuant software). The X-ray spectra were quantified as oxide weight percent stoichiometrically; in all cases it was assumed that iron was present as magnetite (rather than wüstite or hematite). Analyses were carried out on 3 to 6 different areas (typically 100 by 200 microns across but occasionally smaller) on each sample (results normalised to 100wt%) and averaged to give an overall chemical composition for each sample. Analyses were also attempted on individual phases using the SEM in spot mode. However, the interaction volume was typically 5 microns in diameter and some phases, in particular the fayalite and/or glass along iron oxide grain boundaries, could not therefore be analysed in this way. The methods used to characterise the microstructure and chemical composition were identical for both archaeological assemblages and for the hammerscale recovered from the replication experiments.

Archaeological samples of hammerscale

Twenty samples of hammerscale from archaeological contexts were selected for detailed examination and chemical analysis. The samples came from two sites: Mont Beuvray (ancient *Bibracte*), a late Iron Age *oppidum* in central France (Guichard, *et al* 2003), and Hythe Hill, a late medieval smithy in Colchester, Essex (Brooks 2000). The samples from both sites were taken from the *in situ* floor surfaces of workshops used for working iron (smithies).

Table 1. Archaeological samples of hammerscale

Samples	Site	Form
A1–A5	Mont Beuvray	Flake
A6–A10	Mont Beuvray	Spheroid
A11–A15	Hythe Hill	Flake
A16–A20	Hythe Hill	Spheroid

Examination of hammerscale from Mont Beuvray, France

The excavation of a late Iron Age blacksmith's workshop on Mont Beuvray, France (ancient Bibracte) provided the opportunity to collect samples of hammerscale (Guichard, *et al* 2003). Hundreds of samples were taken on a grid through the workshop following the methodology described by Mills and McDonnell (1992). Samples of flake and spheroidal hammerscale (5 samples of each) representative of the whole assemblage were selected for detailed examination and chemical analysis.

Flake hammerscale

The samples of flake hammerscale from Mont Beuvray are composed almost entirely of large, euhedral grains of iron oxide, with a very small amount of a second phase (possibly fayalite), usually along the iron oxide grain boundaries (Figure 3). The microstructure agrees with the model for formation: the surface of oxidation of the solid iron. In most cases the iron oxide grains are probably magnetite but the SEM images (back scatter detector) show occasional differences in brightness which probably reflect the fact that some of the iron oxide is present as wüstite and/or hematite. The arrangement of the iron oxide grains in the flake hammerscale often shows a series of layers. It is possible that each layer reflects a heating episode.

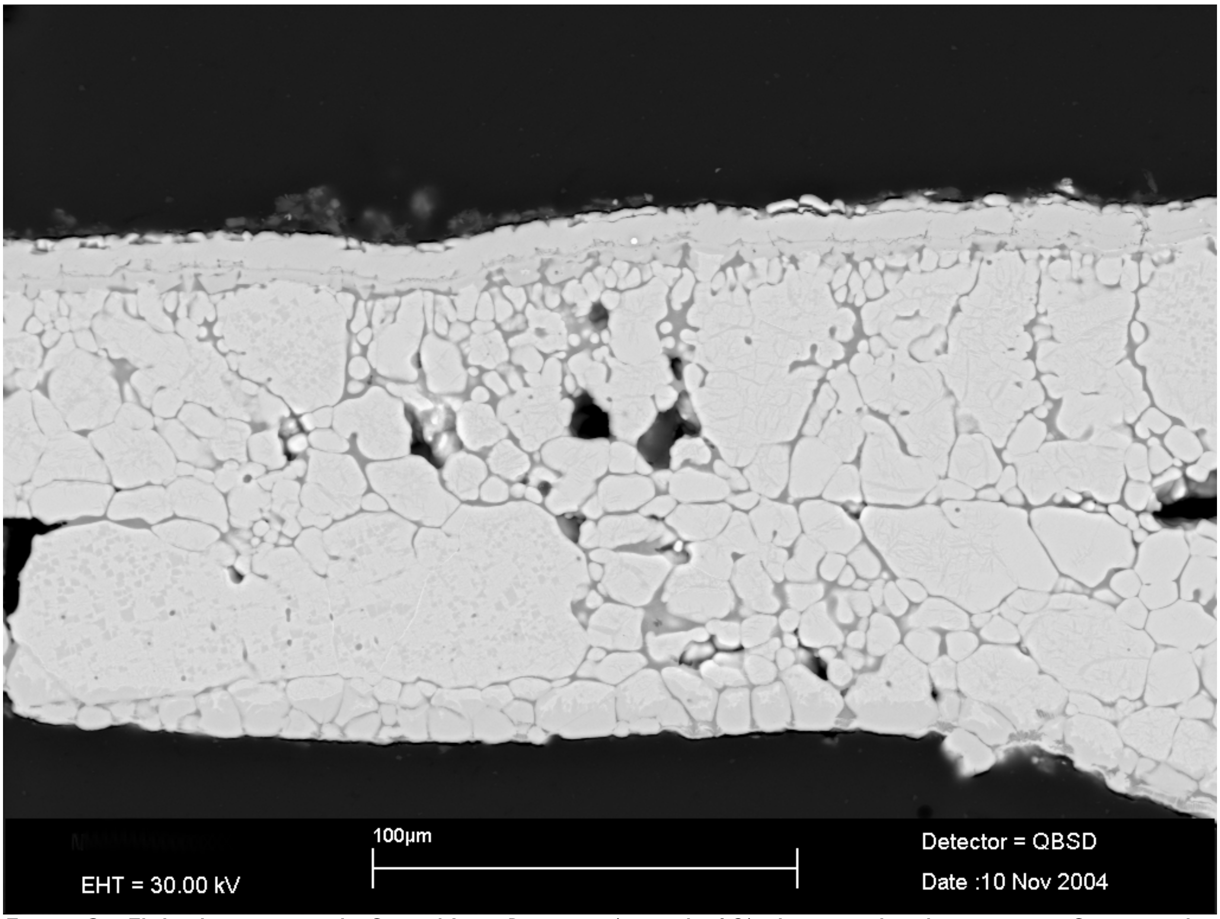

Figure 3. Flake hammerscale from Mont Beuvray (sample A2) showing the dominance of iron oxide with some fayalite or glassy material along grain boundary

The chemical composition of the flake hammerscale from Mont Beuvray reflects the microstructure described above: it is rich in iron oxide (Table 2). Calculated as magnetite, the iron oxide content of these samples always exceeds 92wt%; the balance comprising mostly silica and alumina.

Table 2. Average composition of the Mont Beuvray flake hammerscale samples (each sample analysed 3–6 areas)

	Na_2O	MgO	Al_2O_3	SiO_2	P_2O_5	SO_3	K_2O	CaO	TiO_2	MnO	Fe_3O_4
A1	<0.1	<0.1	0.7	0.7	<0.1	<0.1	0.1	<0.1	<0.1	<0.1	98.5
A2	<0.1	<0.1	2.2	4.6	<0.1	<0.1	0.3	<0.1	<0.1	<0.1	93.0
A3	<0.1	0.3	2.5	3.5	0.5	<0.1	0.2	0.6	0.1	<0.1	92.2
A4	<0.1	<0.1	0.2	0.2	0.1	<0.1	<0.1	0.1	<0.1	<0.1	99.2
A5	<0.1	<0.1	1.2	2.5	0.3	<0.1	0.2	0.4	<0.1	<0.1	95.5

Spheroidal hammerscale

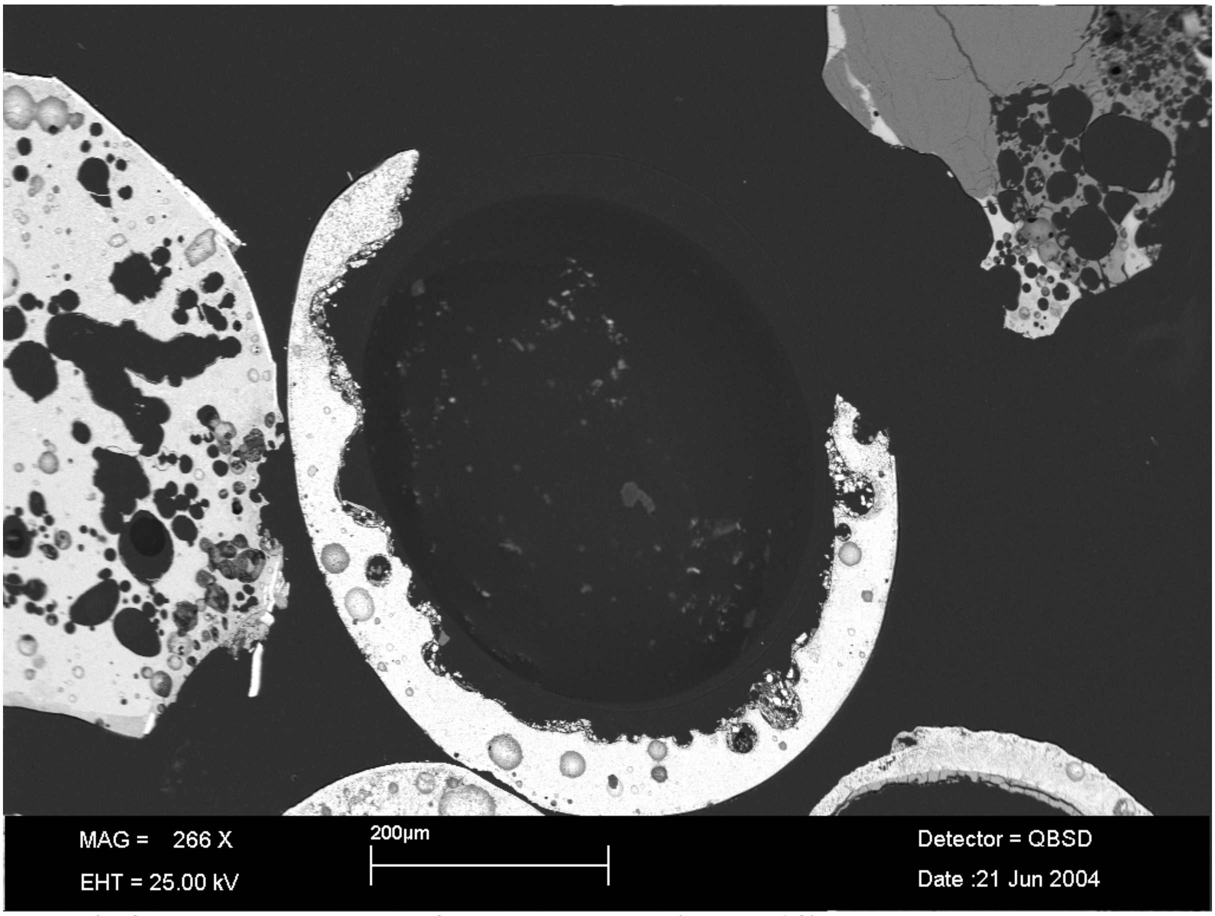

Figure 4. Spheroidal hammerscale from Mont Beuvray (sample A8).

Two of the samples of spheroidal hammerscale from Mont Beuvray (A6 and A8) are hollow (the volume of the cavity is more than half the total volume of the spheroid, Figure 4) but all contain at least some porosity. The samples have a microstructure that is distinct from the flake hammerscale. The spheroids are composed of fine dendrites of iron oxide in a matrix of fayalite and/or glass (Figure 5). The microstructure of the Mont Beuvray spheroidal hammerscale (large iron oxide dendrites with small arm spacing) suggests rapid cooling from liquid to solid. The proportion of fayalite and/or glass in the spheroids is higher than that seen in the flakes. The spheroidal hammerscale from Mont Beuvray has a lower iron oxide content compared to the flake (<92wt%) and higher levels of silica, alumina and lime (see Table 3 and Figure 6).

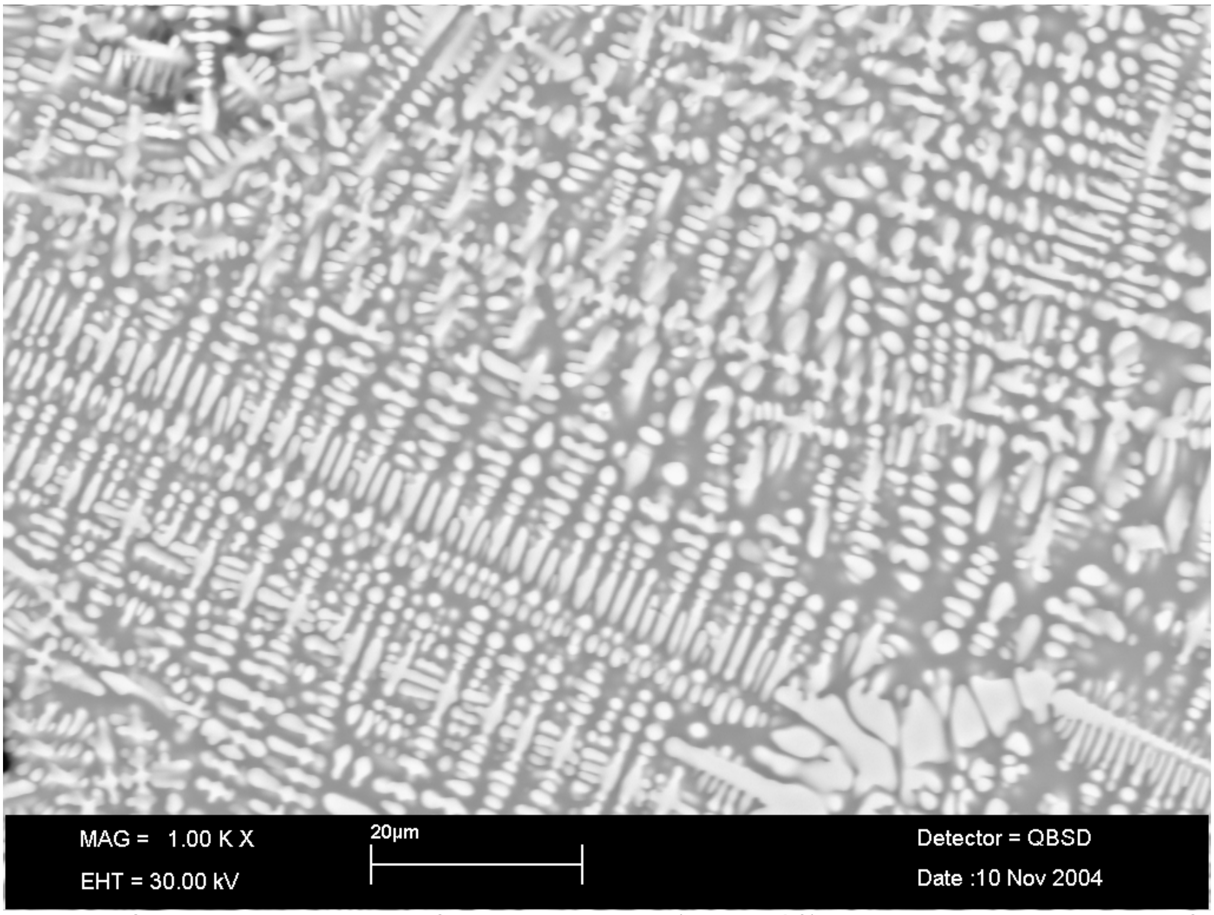

Figure 5. Spheroidal hammerscale from Mont Beuvray (sample A9). The microstructure consists of dendrites of iron oxide in a fayalite(?) matrix

Table 3. Average composition of the Mont Beuvray spheroidal hammerscale samples (each sample analysed 3–6 areas)

	Na_2O	MgO	Al_2O_3	SiO_2	P_2O_5	SO_3	K_2O	CaO	TiO_2	MnO	Fe_3O_4
A6	<0.1	<0.1	2.0	6.4	0.2	<0.1	0.2	0.1	<0.1	<0.1	91.1
A7	<0.1	<0.1	2.9	7.4	0.4	<0.1	0.3	0.1	<0.1	<0.1	88.9
A8	<0.1	<0.1	2.7	7.4	0.4	<0.1	0.2	0.2	<.1	<0.1	89.1
A9	<0.1	<0.1	5.7	13.8	0.3	<0.1	1.1	0.9	<0.1	0.1	77.9
A10	<0.1	<0.1	2.3	6.4	0.1	<0.1	0.3	<0.1	<0.1	0.5	90.4

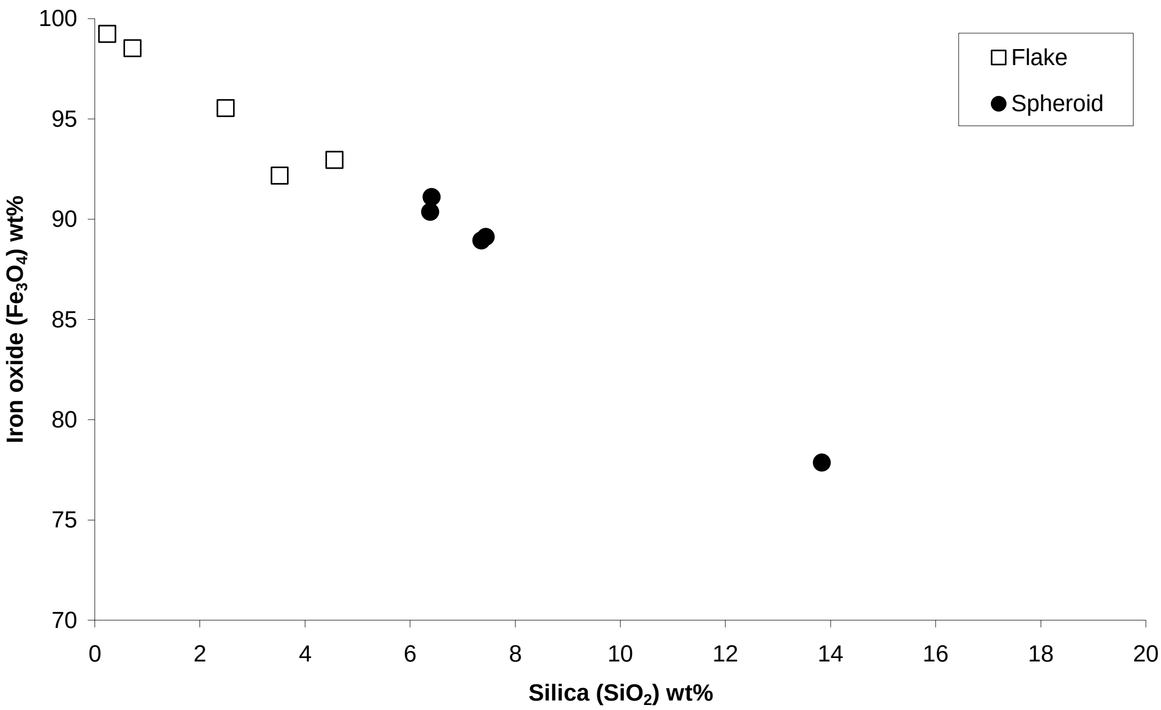

Figure 6. Iron oxide and silica content of hammerscale from Mont Beuvray

Examination of hammerscale from Hythe Hill, Colchester

The excavation of a late medieval (15th- or 16th-century) smithy at 79 Hythe Hill, Colchester (Brooks 2000) recovered substantial quantities of smithing pan, consisting of a floor deposit of hammerscale cemented together. A sample of this smithing pan was immersed in water in an ultrasonic tank to disaggregate it. Samples of flake and hammerscale representative of the whole assemblage were selected for detailed examination and chemical analysis.

Flake hammerscale

The samples of flake hammerscale from Hythe Hill (Figure 7) display similar microstructures to those seen from Mont Beuvray (see above). There are large, euhedral grains of iron oxide, with a very small amount of a second phase, usually along the iron oxide grain boundaries. The iron oxide grains are again often present as a series of layers. The chemical analysis of the Hythe Hill flake hammerscale (Table 4) shows that they are rich in iron oxide (>95wt% calculated as magnetite).

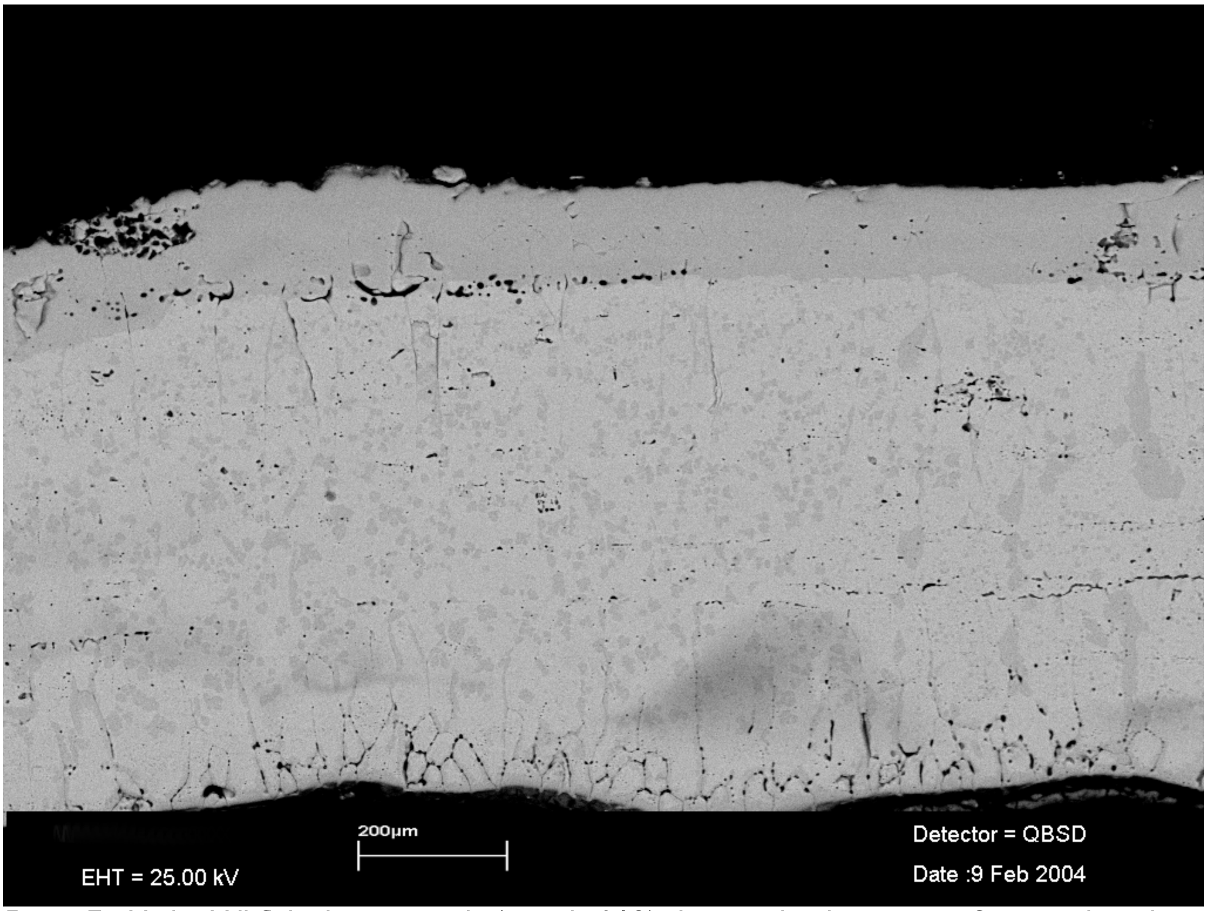

Figure 7. Hythe Hill flake hammerscale (sample A12) showing the dominance of iron oxide with some fayalite or glassy material along grain boundaries. The slight differences in brightness for the iron oxide may reflect the presence of different oxides, eg wüstite and magnetite. Analyses of individual spots suggests that there is also some substitution of Al_2O_3 in the magnetite

Table 4. Average composition of the Hythe Hill flake hammerscale samples (each sample analysed 3–6 areas)

	Na_2O	MgO	Al_2O_3	SiO_2	P_2O_5	SO_3	K_2O	CaO	TiO_2	MnO	Fe_3O_4
A11	<0.1	<0.1	0.5	2.5	0.3	<0.1	<0.1	0.2	<0.1	<0.1	96.4
A12	<0.1	<0.1	0.2	0.2	<0.1	<0.1	<0.1	0.2	<0.1	<0.1	99.4
A13	<0.1	0.1	1.0	2.8	0.1	<0.1	0.1	0.4	<0.1	<0.1	95.4
A14	0.3	<0.1	0.4	1.1	0.9	<0.1	0.1	0.7	<0.1	<0.1	96.4
A15	<0.1	<0.1	0.4	0.5	<0.1	<0.1	<0.1	0.1	<0.1	<0.1	98.9

Spheroidal hammerscale

The majority of samples of spheroidal hammerscale from Hythe Hill had some voids within, some of which were small compared to the overall size of the spheroid, but one comprised just an outer shell. The microstructures are similar to those from Mont Beuvray discussed above: fine dendrites of iron oxide in a matrix of fayalite and/or glass. The spheroidal hammerscale from Hythe Hill has a variable chemical composition. Three samples (A17, A18 and A20) contain relatively low levels of iron oxide and high levels of silica, alumina and lime, but two samples (A16 and A19) have compositions that much closer to that of flake hammerscale.

Table 5. Average composition of the Hythe Hill spheroidal hammerscale samples (each sample analysed 3–6 areas)

	Na_2O	MgO	Al_2O_3	SiO_2	P_2O_5	SO_3	K_2O	CaO	TiO_2	MnO	Fe_3O_4
A16	<0.1	<0.1	0.6	3.5	0.4	<0.1	0.1	0.5	<0.1	<0.1	94.9
A17	0.7	0.6	5.7	16.8	0.4	<0.1	1.4	0.8	<0.1	<0.1	73.6
A18	0.4	0.2	6.1	19.3	0.4	<0.1	1.9	0.9	0.1	<0.1	70.6
A19	<0.1	<0.1	0.8	3.7	0.3	<0.1	0.2	0.2	<0.1	<0.1	94.8
A20	<0.1	0.3	3.4	18.4	0.4	<0.1	0.9	1.5	0.2	<0.1	75.0

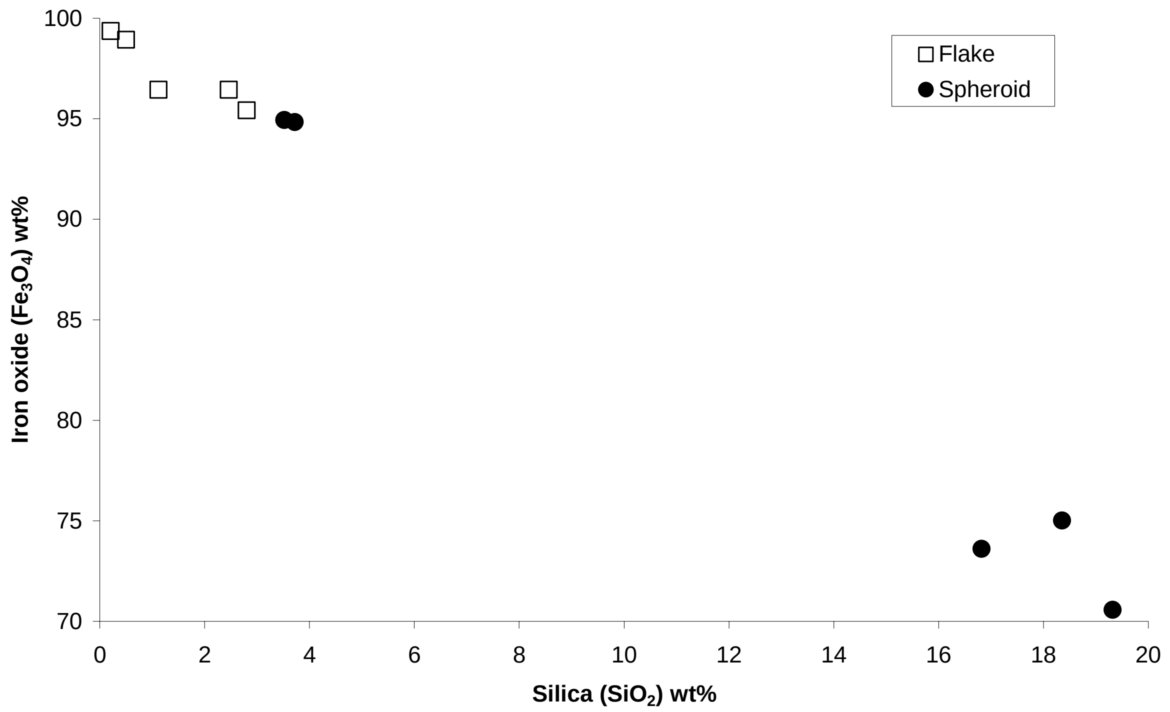

Figure 8. Iron oxide and silica content of hammerscale from Hythe Hill

Discussion of archaeological hammerscale

The examination of the hammerscale samples from Mont Beuvray and Hythe Hill shows that flake hammerscale consists almost entirely of euhedral grains of iron oxide with a small amount of fayalite or glassy material along grain boundaries. This microstructure is compatible with a model in which the iron oxides grow on the surface of the iron, both as solids. The spheroidal hammerscale is often hollow and consists of dendritic iron oxide in a fayalite or glassy matrix. This microstructure is compatible with a model of formation in which the spheroids start as a liquid and solidify during flight. There are no significant differences in the microstructures or compositions of the two types of hammerscale when comparing between the two sites.

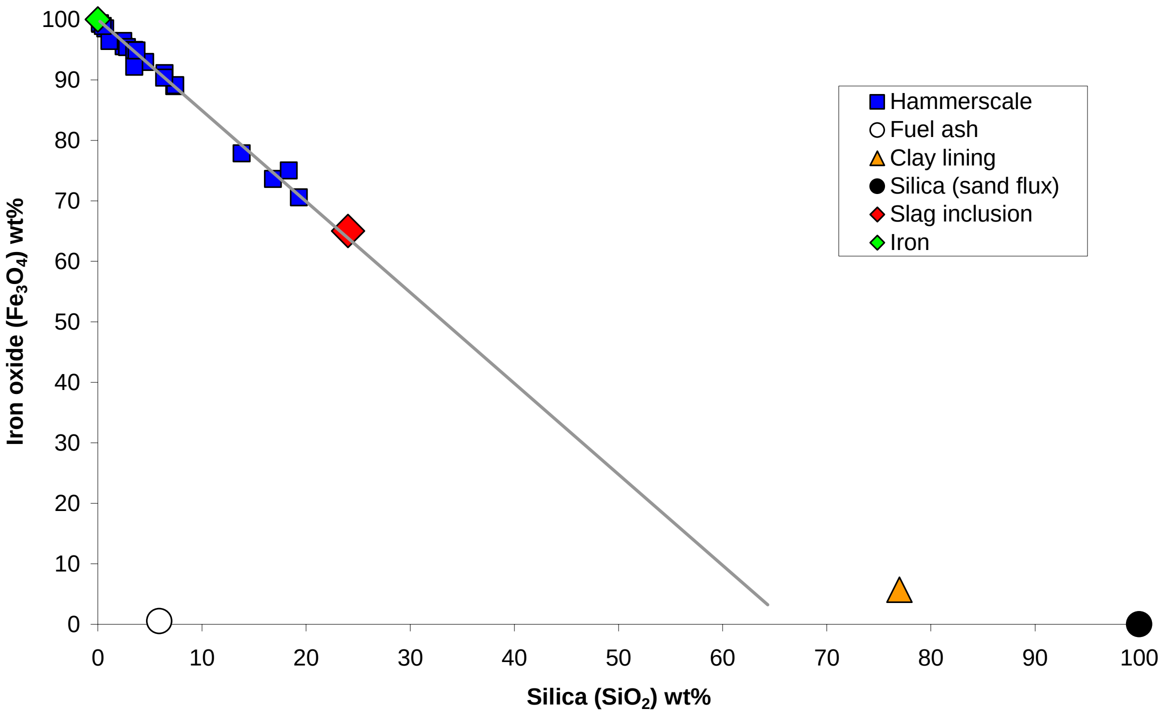

Figure 9. Plot of silica and iron oxide contents for all archaeological samples of hammerscale and the estimated likely compositions of the various inputs

The compositions of the archaeological samples of hammerscale show correlations between most oxides (Figures 9 and 10). These correlations provide information about the role of other materials in the formation of hammerscale. Clearly the most important input is the metallic iron, but the slag inclusions in the metal, silica from any sand flux used, the ash from the fuel used (charcoal), and clay from the lining may also contribute. The chemical compositions of the materials used at Mont Beuvray and Hythe Hill are unknown but approximations have been made. All bloomery iron artefacts contain a small proportion of trapped slag most of which derives from the smelting process. The composition of a typical slag inclusion was obtained by averaging the data from a large body of iron smelting slags (Paynter 2006). The fuel ash composition is an average based on several reported analyses of oak and other hardwoods (Turner 1956; Jackson, *et al* 2005). A typical clay lining composition was obtained by averaging some readily available data (Dungworth forthcoming; Paynter 2002; Starley 2000). The average values of all of the possible inputs are given in Table 6.

Table 6. Average estimated composition of the various possible materials which could form hammerscale

	Na_2O	MgO	Al_2O_3	SiO_2	P_2O_5	K_2O	CaO	TiO_2	MnO	Fe_3O_4
Fuel ash	2.6	6.1	0.5	5.9	6.2	16.9	57.4	0.0	1.2	0.5
Clay lining	0.5	1.1	10.7	77.0	0.4	2.7	0.8	0.9	0.1	5.7
Slag inclusions	0.0	0.8	4.0	24.0	1.3	1.0	1.9	0.2	1.0	65.0
Silica	0.0	0.0	0.0	100.0	0.0	0.0	0.0	0.0	0.0	0.0
Iron	0.0	0.0	0.0	0.0	0.0	0.0	0.0	0.0	0.0	100.0

The plot of alumina and potash (Figure 10) shows that all of the hammerscale samples contain some alumina and potash. The increase in alumina and potash correlates with the silica content. Silica sand would not contain these oxides and so it cannot have been used on its own. It is unlikely that fuel ash was a significant input as it contains excessively high levels of potash and lime. The titanium oxide content of most clay linings (0.9wt%) is too high for this material to have made a significant contribution to the formation of hammerscale (<0.1wt%). The compositional trends for hammerscale are likely to be produced by reactions between metallic iron and the slag inclusions in the metal.

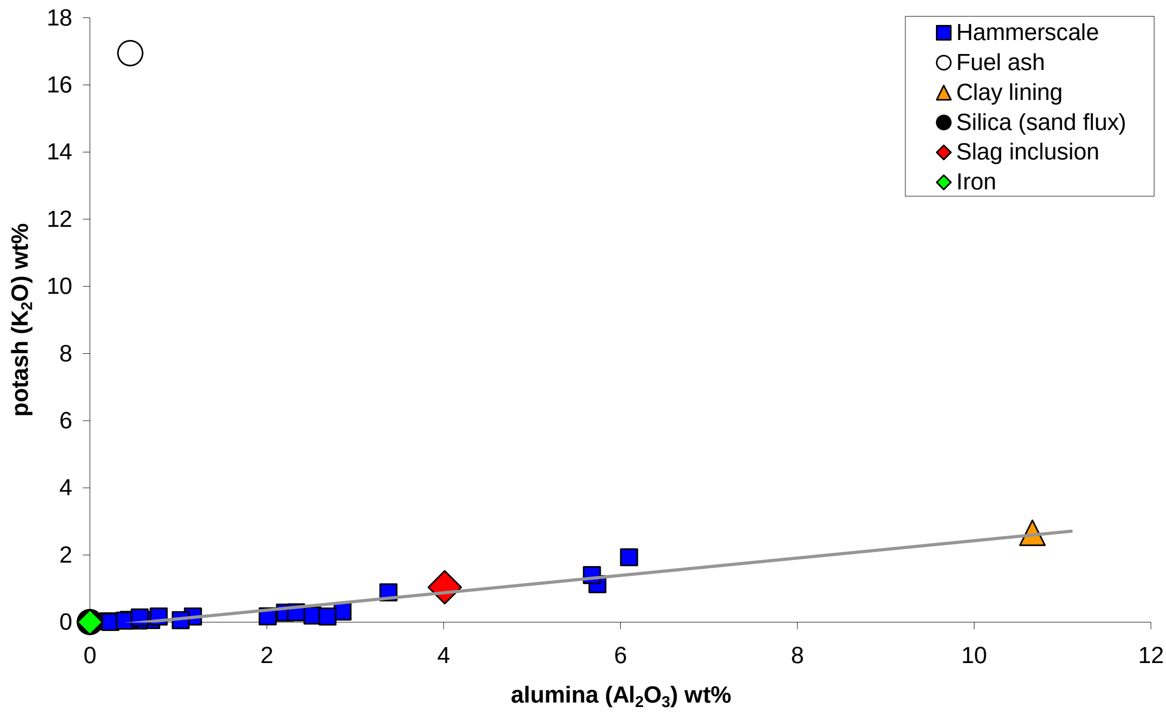

Figure 10. Plot of alumina and potash content for all archaeological samples of hammerscale and the likely composition of the various inputs

Replication experiments

A series of experiments were carried out to examine the types of hammerscale produced during different forging and welding experiments (Figure 11). These were undertaken using modern mild steel and a bar of wrought iron produced by puddling (19th or early 20th century). The wrought iron bar was retained to determine the sorts of non-metallic inclusions present, unfortunately a sample of the steel bar used was not retained. The forging and welding were carried out in the teaching workshops of West Dean College, Chichester, under the supervision of a professional smith (Andrew Breese). The floor around the hearth and anvil (to a distance of 5m) was thoroughly cleaned before work started. After each experiment the hammerscale was swept up and bagged (all material fell within 2m of the anvil). This material was subsequently sorted into flake, spheroidal and miscellaneous hammerscale.

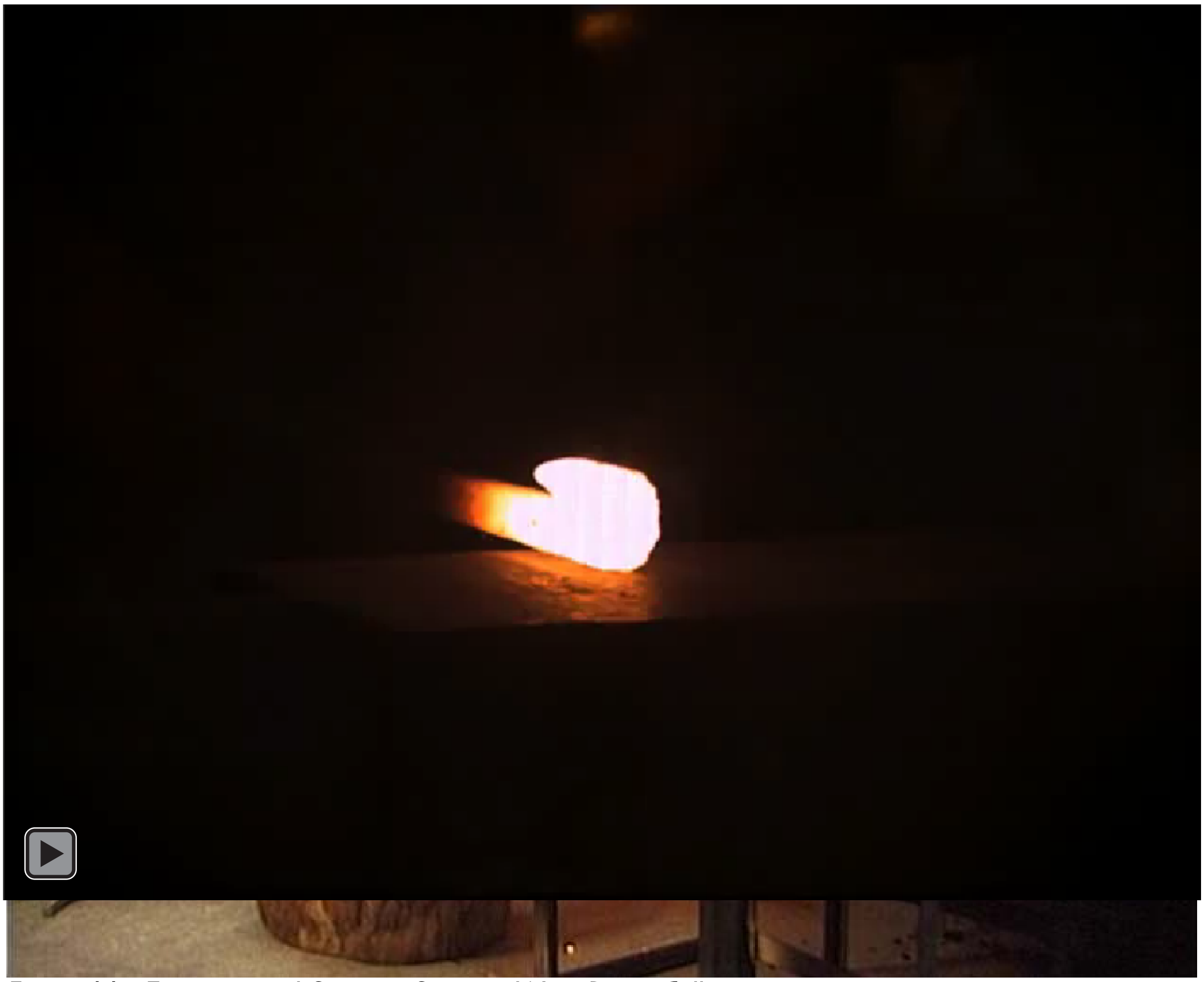

Figure 11. Experimental forging of iron at West Dean College

The blacksmith's hearth was of a modern type (Figure 11). It was constructed from sheet metal and had a water-cooled cast iron tuyère (cf CSIRA 1952, 1–3, Fig 2). The draught was provided by an electric blower and the fuel used was a metallurgical coke (samples of clinker were retained for analysis). The experiments were designed to reproduce traditional forging and welding actions. One end of a bar of iron or steel (each 20mm square-sectioned bars) was forged down to approximately 10mm by 25mm section and then bent back on itself ready for welding. This required up to five separate periods of heating and forging. The welding was achieved by heating the prepared metal to a bright yellow heat and striking with a hammer (cf CSIRA 1952, 21). No fluxes were used during the forging or welding. The welded end of the bar was then forged down and bent back on itself in preparation for the next weld.

In total, 144.4g of hammerscale was recovered from the floor (Table 7); an unknown amount of hammerscale is likely to have been lost in the hearth during heating. Each stage of forging iron produced on average 20.8g of hammerscale while similar forging of mild steel produced only 3.8g. Each stage of welding iron produced on average 3.8g of material while steel produced 4.8g of material. The majority of the miscellaneous material was produced during the working of iron. Each period of forging (each lasting 10–30 minutes) produced on average 14.5g of hammerscale, of which 93% was flake and 1.7% was spheroidal. Each period of welding (up to 1 minute) produced on average 4.3g of hammerscale, of which 79% was flake and 5.8% was spheroidal.

The proportion of spheroidal hammerscale formed during welding always exceeded that of the preceding forging stage. It is striking that almost no spheroidal hammerscale (0.0006g) was recovered from the first period of forging. Examination of this spheroidal material (see below) suggests that none was produced by fire-welding and it is all contamination. It is possible that the spheroidal hammerscale recovered from later forging stages were actually from earlier welding stages (ie contamination). With hindsight the dustpan and brush did not recover all material.

Some spheroidal hammerscale seems to be produced during welding but the proportion of flake hammerscale produced never dropped below 70%. The welding requires the iron to be strongly heated and then struck with a hammer. It is to be expected that welding would still create substantial quantities of flake hammerscale.

The data from the hammerscale samples collected suggests that spheroidal hammerscale is produced by fire-welding and this has been confirmed by the high-speed digital video (see below).

Table 7. Weights of hammerscale recovered from each experiment.

			Weight (g)			Percentage		
Experiment	**Action**	**Metal**	**Flake**	**Spheroid**	**Misc**	**Plate**	**Spheroid**	**Misc**
1	Forge	Iron	33.32	0.0006	0.95	97.2	0.002	2.8
2	Weld	Iron	2.36	0.21	1.84	53.5	4.8	41.7
3	Forge	Iron	15.29	0.74	0.52	92.4	4.5	3.1
4	Forge	Iron	5.27	0.05	0.05	98.1	0.9	0.9
5	Weld	Iron	3.28	0.19	0.98	73.7	4.3	22.0
6	Forge	Iron	38.34	0.73	3.68	89.7	1.7	8.6
7	Forge	Mild steel	3.21	0.05	0.09	95.8	1.5	2.7
8	Weld	Mild steel	5.61	0.22	0.04	95.6	3.7	0.7
9	Forge	Mild steel	3.36	0.10	0.15	93.1	2.8	4.2
10	Weld	Mild steel	5.04	0.17	0.33	91.0	3.1	6.0
11	Forge	Mild steel	3.93	0.11	0.44	87.7	2.5	9.8
12	Weld	Mild steel	2.25	0.28	0.37	77.6	9.7	12.8
13	Burn	Iron	0.00	1.93	0.00	0.0	100.0	0.0
14	Burn	Mild steel	0.00	1.11	0.00	0.0	100.0	0.0
15	Forge	Iron	4.54	0.15	0.58	86.1	2.8	11.0
16	Weld	Iron	1.87	0.41	0.27	73.3	16.1	10.6
Total			**127.67**	**6.45**	**10.29**	**88.4**	**4.5**	**7.1**

In addition to forging and welding the wrought iron and mild steel, samples of both metal were over-heated until they began to burn. There was no control over the temperature of the burning; samples were simply heated until they began to resemble sparklers (Figure 12). The material which spontaneously fell off the metal, all of which was spheroidal, was collected in a container (Figure 12). These combustion spheroids are generally larger than the spheroidal material produced by fire-welding and subsequent examination (see below) shows there are other distinctive features to this sort of material.

Figure 12. An over-heated bar of iron with the spheroidal material collected in a container

A conventional digital video camera (25 frames per second) was used to record the action for the duration of all the experiments (Figure 11, see also the CD which accompanies this report, lowspeed.avi). In addition a high-speed digital camera (600 frames per second) was used to record several seconds of action for each welding experiment (see the CD which accompanies this report, highspeed.avi). A series of stills from this video are reproduced as Figures 13–17. Figure 13 illustrates the difficulties of capturing high-speed digital images; indeed the image is only intelligible because of the incandescent light provided by the bar of iron to be welded. This light shows up the surface of the anvil below and the hammer above as it is about the fall onto the bar of iron. The hammer weighs about 500g and just prior to the impact was travelling at approximately $3ms^{-1}$. Figure 14 shows the welding 1 frame (1/600th of a second) after the moment of impact. The outline of the bar of iron has become lost as much of the oxidised surface of the bar has been dislodged by the force of the hammer blow.

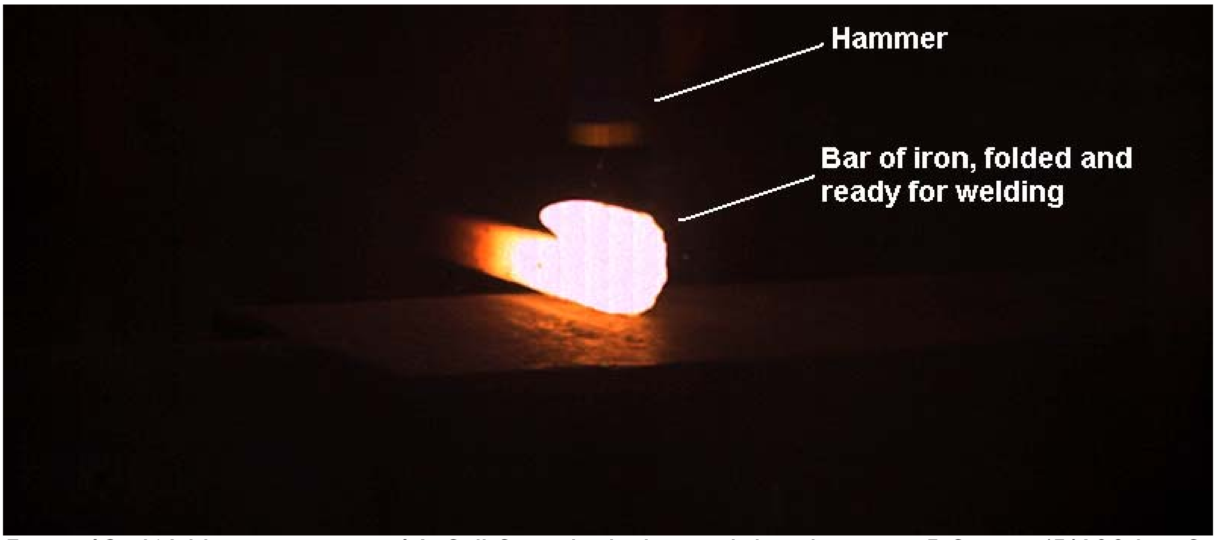

Figure 13. Welding experiment 16. Still from the high-speed digital camera 5 frames (5/600ths of a second) before the impact

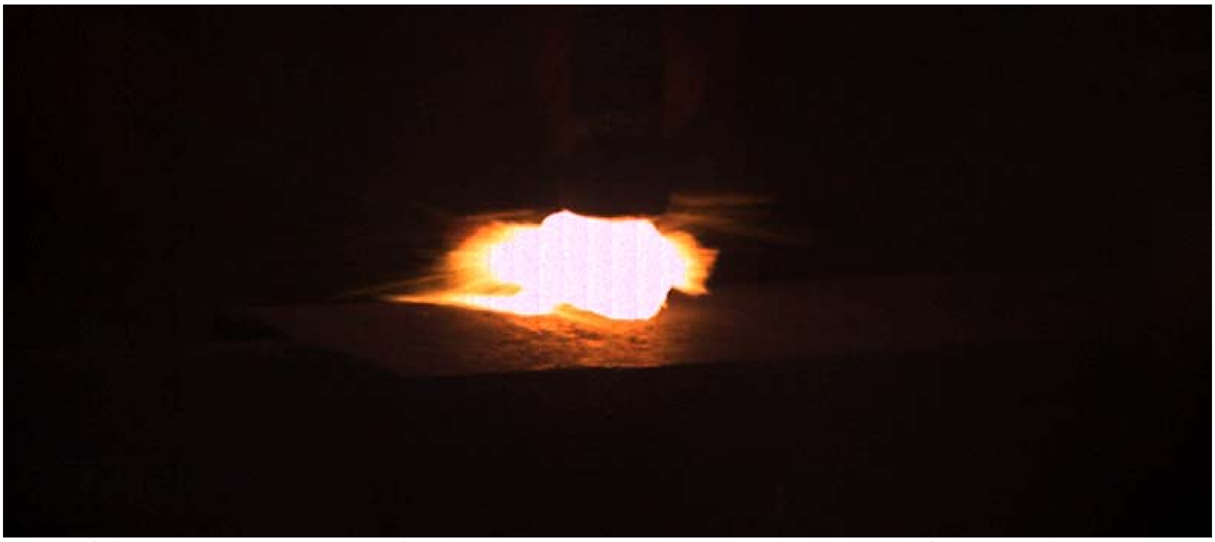
Figure 14. Welding experiment 16. Still from the high-speed digital camera 1 frame after the moment of impact

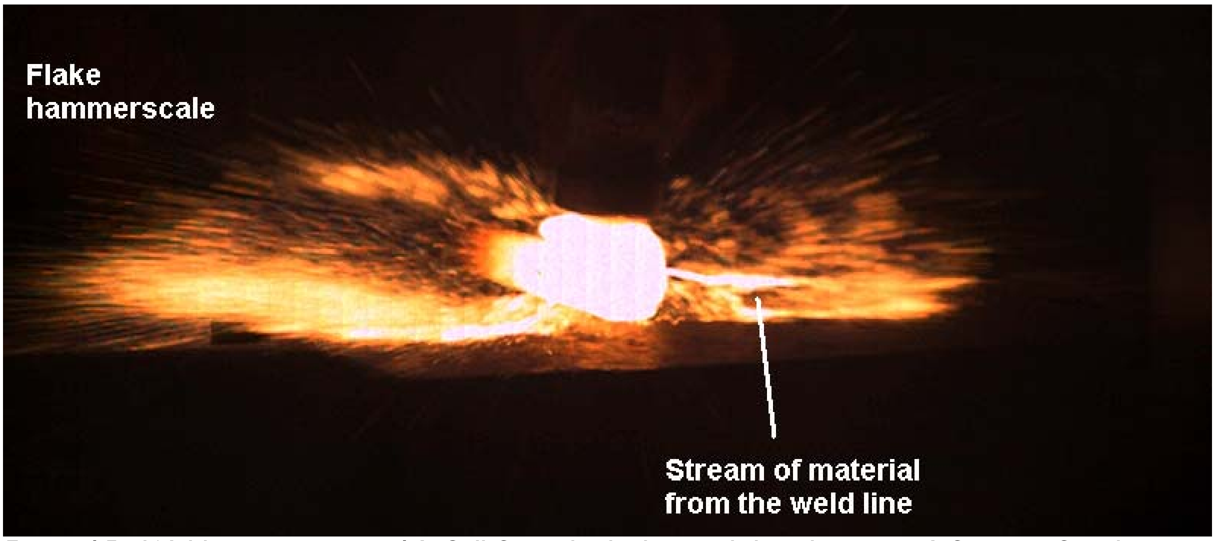

Figure 15. Welding experiment 16. Still from the high-speed digital camera 6 frames after the impact

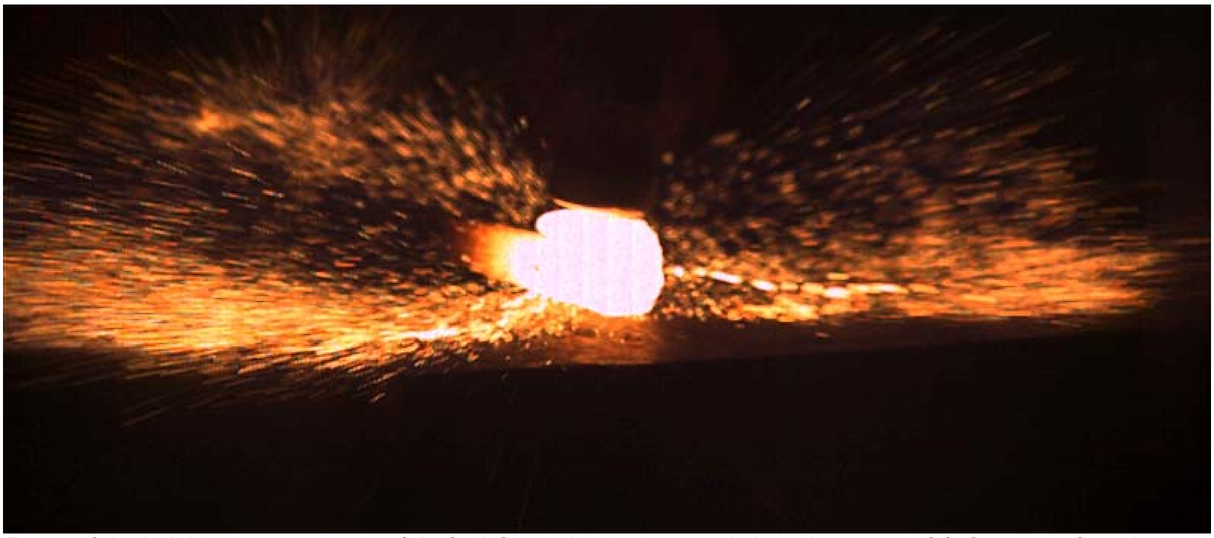

Figure 16. Welding experiment 16. Still from the high-speed digital camera 11 frames after the impact

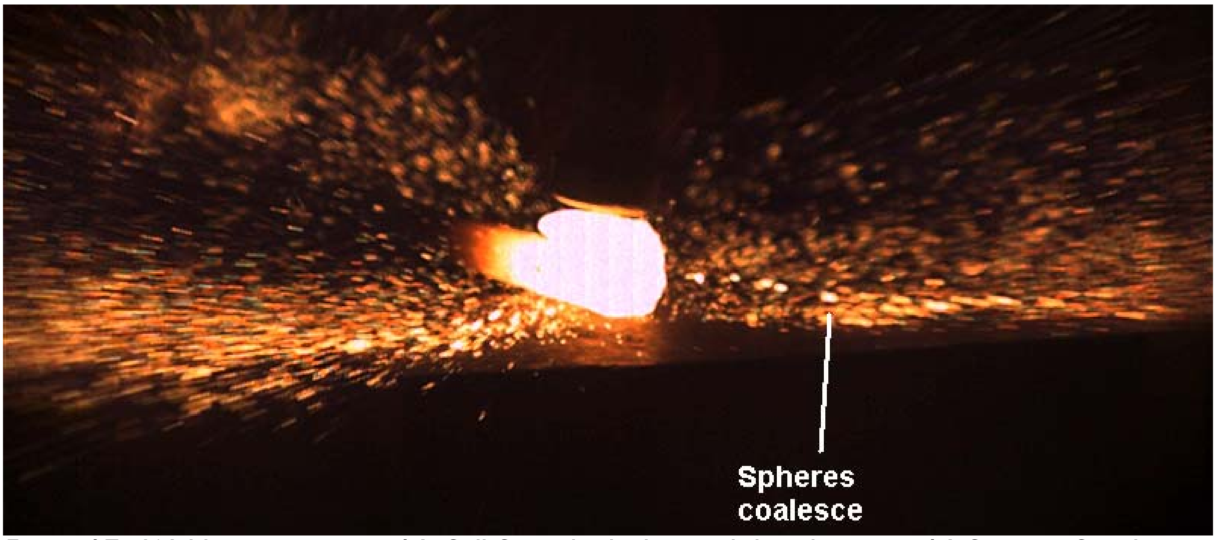

Figure 17. Welding experiment 16. Still from the high-speed digital camera 16 frames after the impact

Figure 15 shows the weld 6 frames after the moment of impact: most of the hammerscale is moving quickly away from the point of impact to produce a shower of sparks similar to Figure 11. In addition, a stream of bright material can be seen emerging from the weld line. The form of this material in this and later frames suggests that as it emerges from the weld line it is molten. In Figure 16 (11 frames after the moment of impact) the stream of material seen in Figure 14 starts to break up into smaller portions. This process is continued in Figure 17 (16 frames, or 0.03 seconds, after the impact) where the stream has broken up and the material has coalesced into a series of spheroids.

The high-speed digital camera has successfully captured the formation of spheroidal hammerscale. The previously proposed model suggested that spheroidal hammerscale was formed during welding. The flake hammerscale within the zone to be welded (plus possibly some flux) was melted by a combination of temperature and pressure and then emerged from the weld as a liquid. The high-speed digital video has shown that this process takes less than 0.03 seconds and would not be observable without the aid of such technology. It has also confirmed the production of considerable quantities of flake hammerscale (cf table 7).

Examination of experimental samples

The examination of the hammerscale produced during the experimental replication of forging and welding provides information about the ways in which the hammerscale formed. The experimental hammerscale was produced under experimental conditions and the (broad) processes which produced each (forging or welding) were controlled (Table 8).

Table 8. Samples of hammerscale selected from the replication experiments (cf Table 6) for detailed analysis

Samples	Experiment	Metal	Action	Type
E1–E6	1	Iron	Forge	Flake
E7–E9	1	Iron	Forge	Spheroid
E10–E15	1	Iron	Forge	Misc
E16–E21	2	Iron	Weld	Spheroid
E22–E24	2	Iron	Weld	Flake
E25	2	Iron	Weld	Misc
E26–E28	5	Iron	Weld	Misc
E29–E31	7	Steel	Forge	Spheroid
E32–E37	7	Steel	Forge	Flake
E38–E43	8	Steel	Weld	Flake
E44–E52	8	Steel	Weld	Spheroid
E53–E55	13	Iron	Burn	Spheroid
E56–E58	14	Steel	Burn	Spheroid

The detailed examination of hammerscale samples reveals that a small proportion were contamination. The most telling example of this is the spheroidal hammerscale from the first stage of forging (samples E7–9), which includes a fragment of cast iron and a titanium-rich glassy material. With hindsight it can be seen that the collection of hammerscale by sweeping the floor was not completely efficient and allowed some hammerscale from previous experiments to be incorporated, and in some cases (as here) debris from earlier activities in the workshop.

In order to aid the interpretation of the material from the forging and welding experiments, the first samples reported on are from the burning experiments. The hammerscale collected from these experiments were the most reliably associated with a particular experiment as the white hot metal was held inside a metal bin while the metal burnt with little or no chance of contamination (cf Figure 12).

Combustion spheroids (Experiments 13 and 14; Samples E53–E58)

The three samples of spheroidal hammerscale from the combustion of the mild steel (samples E56–E58) all have identical microstructures, they consist of a small particle of metallic iron 1–2mm across, surrounded by a film of oxidised material (Figure 18). The core of metallic iron appears to be more-or-less pure iron: there are no areas of carbon or iron-carbides and SEM-EDS analysis could not detect any phosphorus. The surrounding oxidised film is rich in iron oxide and can be distinguished from almost all other samples examined by the high manganese content (on average MnO = 3.6wt%). The microstructure resembles that observed by Starley for Roman spheroidal hammerscale from Creeton Quarry (Starley 1997). This microstructure was also observed in samples E9, E30, and E31 (metal forging experiments) and presumably indicates accidental burning of the metal in these experiments.

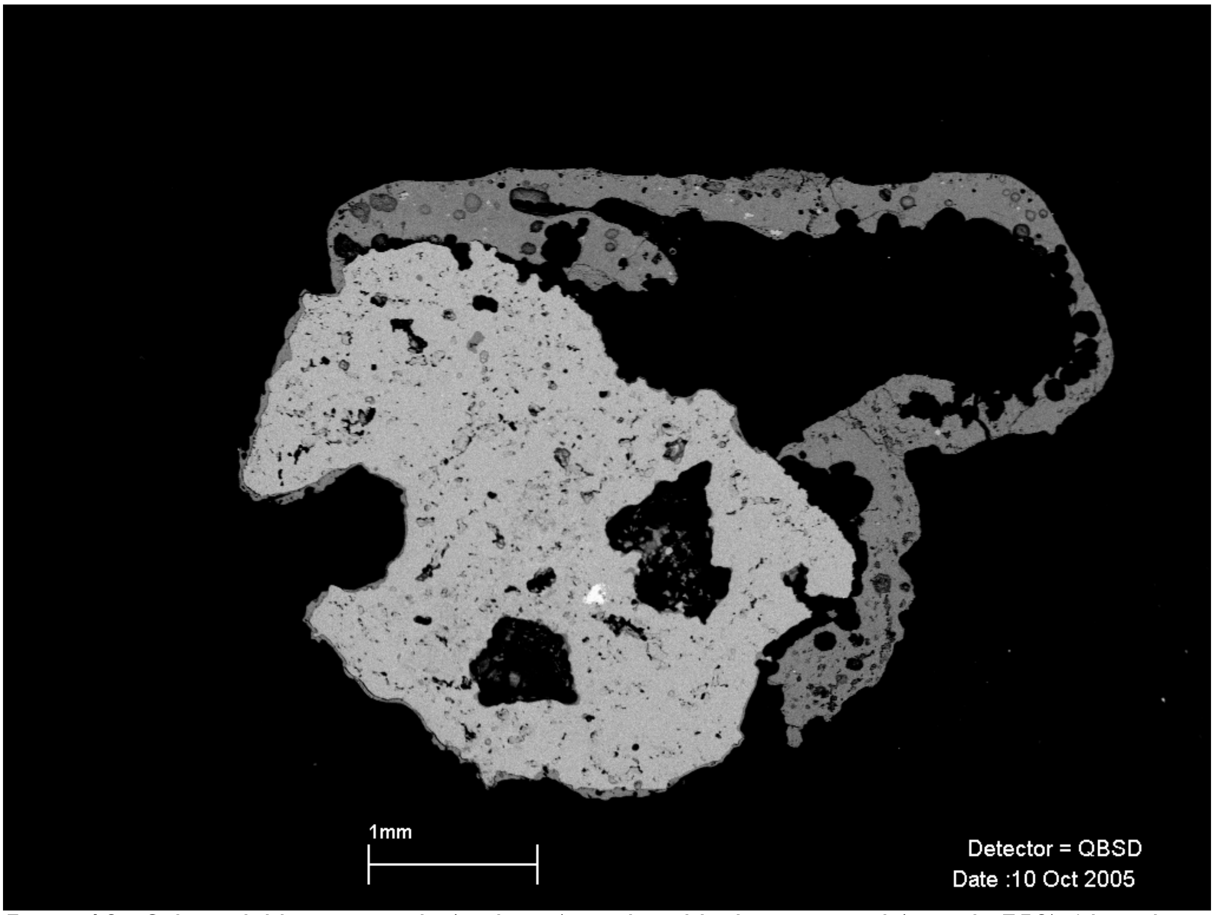

Figure 18. Spheroidal hammerscale (mid grey) produced by burning steel (sample E58). Note the hollow shell is formed of iron oxide and iron silicate with a small core of metallic iron (light grey)

Table 9. Average composition of the spheroidal hammerscale samples produced by burning (combustion) of wrought iron (E53–55) and steel (E56–58). Each sample analysed 3–6 areas

	Na_2O	MgO	Al_2O_3	SiO_2	P_2O_5	SO_3	K_2O	CaO	TiO_2	MnO	Fe_3O_4
E53	0.4	0.2	2.6	12.4	1.3	2.6	0.1	0.3	0.2	0.2	79.8
E54	0.3	0.2	2.3	8.3	0.9	1.8	0.1	0.2	0.2	0.2	85.5
E55	0.5	0.2	2.5	8.2	0.9	1.8	0.1	0.2	0.1	0.2	85.2
E56	0.4	0.3	2.3	7.3	<0.1	2.2	0.1	0.3	0.1	1.8	85.2
E57	0.4	0.2	2.2	5.7	0.2	2.2	<0.1	0.3	0.1	3.7	84.9
E58	0.4	0.3	3.4	9.7	<0.1	2.1	<0.1	0.6	0.2	5.5	77.6

The three samples of spheroidal hammerscale from the combustion of the wrought iron (samples 53–55) have microstructures and compositions which resemble those produced by fire-welding wrought iron; they do not contain metallic iron cores. Some of the examples of spheroidal hammerscale from other experiments (see below) have microstructures which resemble the spheroids produced by burning steel but have oxide films with compositions which resemble the spheroids produced by welding wrought iron.

Flake hammerscale (Samples E1–6, E22–24, E32–43)

Twenty-one samples of flake hammerscale were selected from the forging and welding of both iron and steel. They all displayed the same microstructure: relatively large grains of iron oxide (magnetite?) with small amounts of fayalite or glassy matrix along some grain boundaries (Figure 19). The iron oxide grains in many samples were arranged in layers which might suggest that the flake hammerscale grew episodically. The microstructure of the flake hammerscale seems to be the same regardless of the material (mild steel or wrought iron) or the process (forging or welding). A plot of the phosphorus and manganese shows that there are two compositional groups which are produced from steel on the one hand and wrought iron on the other (Figure 20). The single exception is probably contamination, that is a sample of flake that is actually from an earlier stage of work. Sample E41 was collected after the welding of steel but it has a composition unlike the other steel samples. It has a composition which shows more similarities with the flake hammerscale produced by working wrought iron.

As discussed below, the manganese and phosphorus in these samples of hammerscale is thought to derive principally from the non-metallic inclusions in the metals (slag in the wrought iron and manganese sulphide in the steel). The compositions of the flake hammerscale produced during forging or welding the same metal show few significant differences.

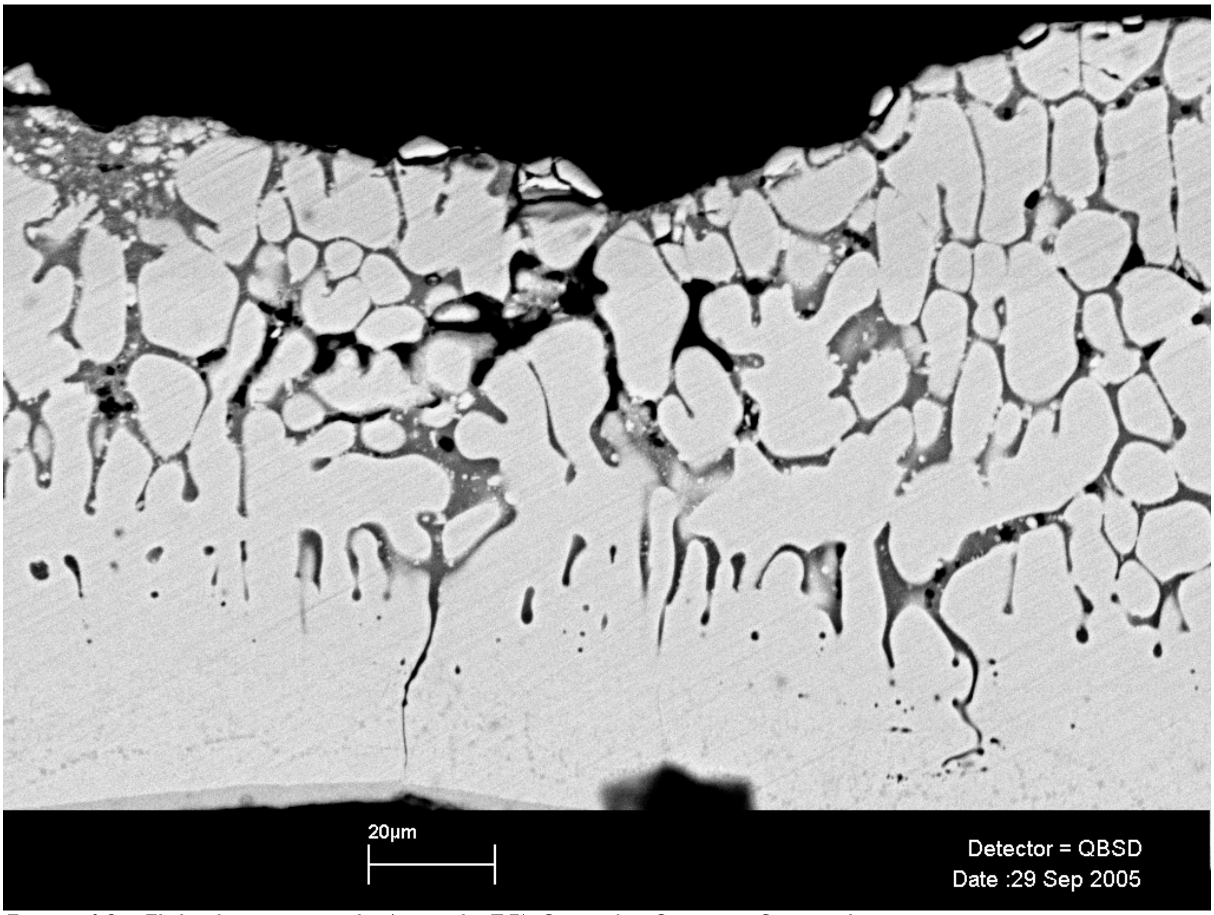

Figure 19. Flake hammerscale (sample E5) from the forging of wrought iron

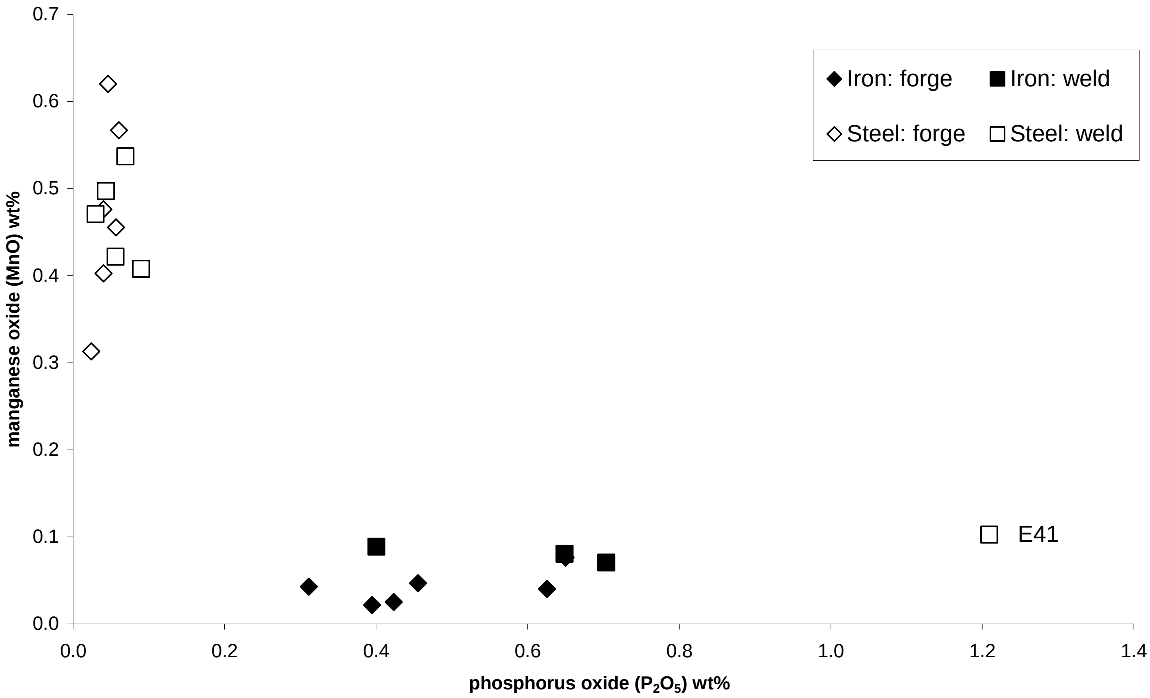

Figure 20. Manganese and phosphorus content of the flake hammerscale. This suggests that sample E41 is contamination

Table 10. Average composition of the flake hammerscale samples (see table 8 for details of the sample). Each sample analysed 3–6 areas

	Na_2O	MgO	Al_2O_3	SiO_2	P_2O_5	SO_3	K_2O	CaO	TiO_2	MnO	Fe_3O_4
E1	0.5	0.1	0.9	2.1	0.5	2.0	<0.1	0.1	<0.1	<0.1	93.6
E2	0.5	0.2	1.7	3.9	0.4	1.6	0.1	0.1	0.2	<0.1	91.3
E3	0.7	0.1	1.1	4.5	0.7	2.4	0.2	0.5	0.2	<0.1	89.6
E4	0.3	0.1	0.7	1.7	0.4	2.2	<0.1	<0.1	<0.1	<0.1	94.4
E5	0.5	0.2	1.6	3.8	0.6	2.6	<0.1	0.2	0.1	<0.1	90.2
E6	0.2	<0.1	1.0	1.7	0.3	1.7	<0.1	<0.1	<0.1	<0.1	94.8
E22	0.1	0.2	0.6	1.2	0.4	0.7	<0.1	<0.1	0.1	<0.1	96.5
E23	0.5	0.1	1.5	4.3	0.7	1.8	<0.1	0.2	0.1	<0.1	90.6
E24	0.3	0.1	0.8	2.0	0.6	1.2	<0.1	0.1	<0.1	<0.1	94.6
E32	0.4	<0.1	0.9	1.7	<0.1	0.9	<0.1	0.1	<0.1	0.4	95.3
E33	0.5	<0.1	0.9	2.7	<0.1	1.7	0.1	0.1	<0.1	0.3	93.4
E34	0.3	<0.1	1.0	1.7	<0.1	1.1	<0.1	0.2	<0.1	0.6	94.9
E35	0.2	<0.1	1.1	2.7	<0.1	0.7	<0.1	0.1	<0.1	0.5	94.5
E36	0.4	<0.1	0.2	0.8	<0.1	1.1	<0.1	<0.1	<0.1	0.6	96.8
E37	0.4	<0.1	1.0	2.1	<0.1	0.8	<0.1	0.1	<0.1	0.5	95.0
E38	0.5	<0.1	0.6	3.6	<0.1	3.3	0.1	0.3	<0.1	0.5	90.8
E39	0.2	<0.1	0.5	1.3	<0.1	2.5	<0.1	<0.1	<0.1	0.4	94.8
E40	0.2	<0.1	0.6	1.6	<0.1	3.5	<0.1	<0.1	<0.1	0.5	93.4
E41	0.9	<0.1	1.1	3.9	1.2	2.4	0.2	0.4	0.1	0.1	89.8
E42	0.9	0.2	1.4	3.8	<0.1	3.4	0.1	0.3	<0.1	0.5	89.3
E43	0.2	0.1	0.8	1.6	<0.1	0.4	<0.1	0.1	<0.1	0.4	96.0

Spheroidal hammerscale (Samples E7–9, E16–21, E29–31, E44–52)

Twenty-one samples of spheroidal hammerscale were selected from the forging and welding of both iron and steel. Unlike the flake hammerscale, the spheroidal hammerscale shows considerable variation in microstructure. In particular, the spheroids collected after some forging experiments are likely to be contamination from earlier experiments.

Table 11. Average composition of the spheroidal hammerscale samples (see table 7 for details) (each sample analysed 3–6 areas). The fragment of cast iron (E7) is not included

	Na_2O	MgO	Al_2O_3	SiO_2	P_2O_5	SO_3	K_2O	CaO	TiO_2	MnO	Fe_3O_4
E8	0.1	0.3	3.3	13.1	0.2	<0.1	1.3	3.8	53.8	9.3	14.7
E9	0.5	0.1	1.0	3.5	1.5	1.8	<0.1	0.3	<0.1	<0.1	91.2
E16	0.7	0.2	2.8	7.6	1.0	3.9	0.1	0.4	0.2	0.1	83.0
E17	0.7	0.3	2.5	9.5	0.9	0.2	0.1	0.5	0.1	<0.1	85.2
E18	0.8	0.4	5.7	15.3	<0.1	6.5	0.5	1.1	0.3	0.6	68.6
E19	1.0	0.4	3.8	14.3	1.9	<0.1	0.2	0.7	0.3	0.3	77.2
E20	1.1	0.5	4.2	15.7	1.2	<0.1	0.2	0.7	0.2	0.1	76.0
E21	1.2	0.4	4.0	14.1	1.1	<0.1	0.3	0.8	0.2	0.1	77.7
E29	0.6	0.4	3.1	8.0	0.6	0.1	<0.1	0.4	0.2	0.1	86.4
E30	0.3	0.1	1.1	4.9	1.6	0.8	<0.1	0.1	0.1	0.4	90.5
E31	0.8	0.3	4.0	12.8	0.8	4.8	0.2	0.6	0.2	0.1	75.4
E44	0.6	0.1	2.5	9.2	0.1	0.9	0.2	0.5	0.2	0.6	85.0
E45	0.6	0.3	3.1	9.8	0.1	0.2	0.3	0.7	0.1	0.5	84.3
E46	0.7	0.3	2.2	6.7	<0.1	2.7	0.2	0.3	0.2	0.5	86.1
E47	0.4	0.2	2.6	7.3	<0.1	2.5	0.1	0.3	0.1	0.8	85.5
E48	0.8	0.4	5.6	15.3	<0.1	1.0	0.4	1.0	0.3	0.6	74.4
E49	1.0	0.5	5.2	15.4	<0.1	0.1	0.5	1.0	0.3	0.5	75.4
E50	0.4	0.1	2.3	5.9	<0.1	2.4	0.1	0.3	0.1	0.5	87.7
E51	0.4	0.3	3.5	9.3	<0.1	1.0	0.2	0.4	0.2	0.6	84.0
E52	1.0	0.4	5.8	14.4	<0.1	<0.1	0.3	0.8	0.3	0.6	76.4

After the first experimental forging of wrought iron, a small amount of spheroidal material was collected (6 spheroids, weighing in total less than 1mg). All three of the spheroids sampled appear to have been produced by burning or are contamination. Sample E7 is a droplet of cast iron (Figure 21). This has carbon present as graphite flakes with no apparent cementite. Chemical analysis suggests a significant proportion of silicon (~5wt%) but no phosphorus, sulphur or manganese were detected. This sample could possibly derive from the tuyère which is made of cast iron. The shape of Sample E8 (Figure 22) suggests that this sample has cooled from a liquid and that as it solidified it had a high surface tension. The chemical composition of this sample (>50wt% titanium oxide) is unlike any of the other samples analysed for this project and suggests arc welding using a rutile flux-cored wire. It is suspected that this material derives from earlier metalworking activity at West Dean.

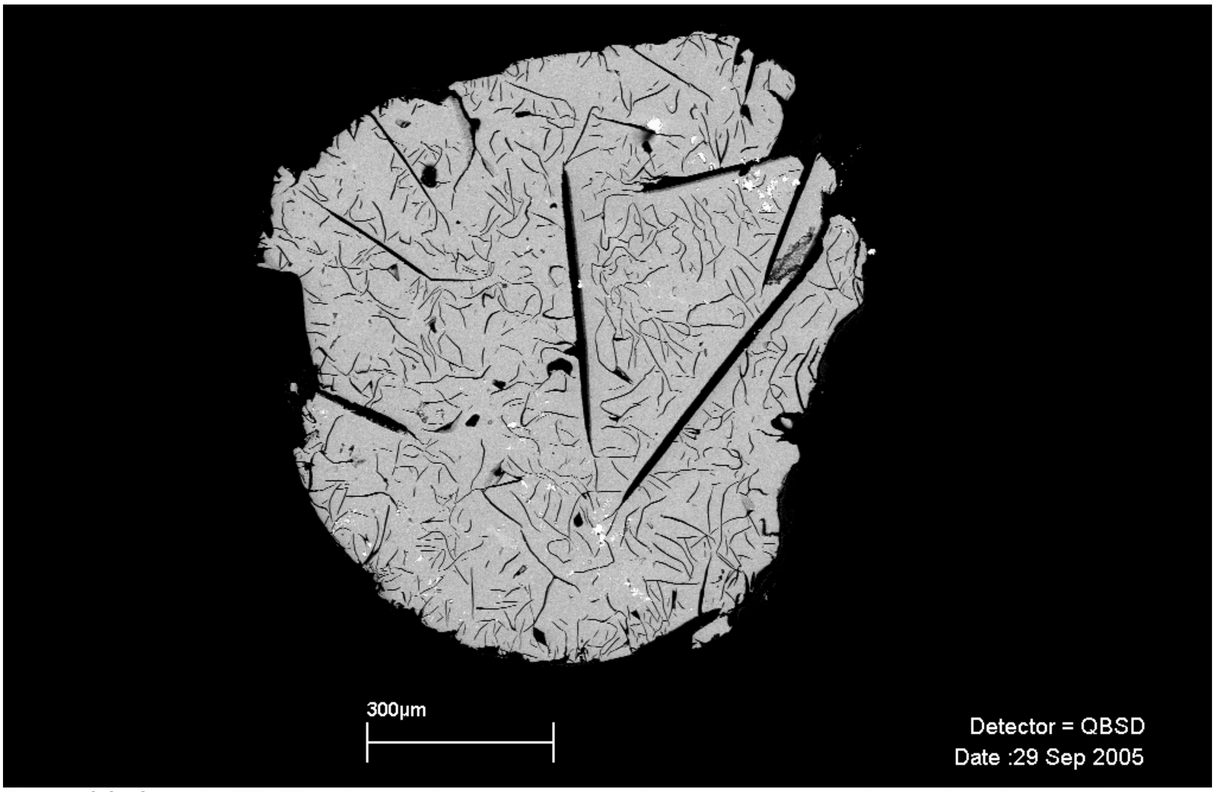

Figure 21. Sample E7. The chemical composition and microstructure indicate that this sample is cast iron. It is possible that it is contamination from the tuyère

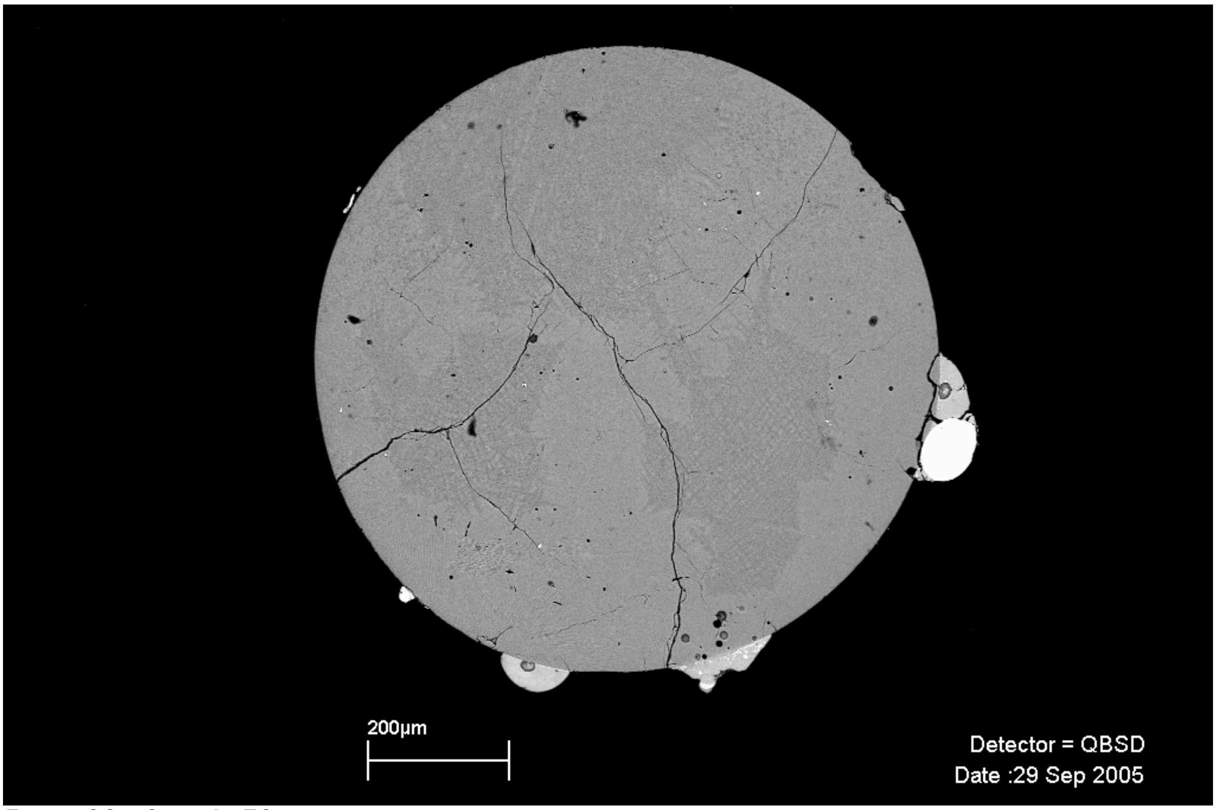

Figure 22. Sample E8

Sample E9 consists of a fragment of metallic iron within an oxide shell (cf Figure 18). This has a microstructure which resembles the spheroidal hammerscale collected during the burning of steel (Samples E56–58) but the oxide shell contains low levels of manganese and relatively high levels of phosphorus. The composition of the oxide shell is similar to the spheroidal hammerscale produced by welding wrought iron. It is possible that this sample was produced by burning wrought iron but it is not clear why it does not have a microstructure similar to that of the spheroids produced by burning wrought iron.

The three spheroids collected after forging mild steel (E29–31) consist of two with metallic iron cores with oxide films (burning spheroids) and one spheroid with a microstructure which resembles those produced by welding (E29). However, all three spheroids have compositions which resemble those produced from wrought iron (ie low manganese and high phosphorus content). Therefore, it is probable that all three spheroids collected after forging mild steel are contamination.

The spheroids collected after welding wrought iron and mild steel all showed a similar microstructure. Most were hollow (Figure 23) and comprised iron oxide (probably magnetite) in a fayalite or glassy matrix. Unlike the archaeological samples, however, the iron oxide is mainly present as small equiaxed euhedral grains rather than dendrites (Figure 24). The presence of euhedral grains rather than dendrites suggests a slower cooling rate compared to the archaeological examples. The differences in microstructure between the experimental spheroids and the archaeological examples could be due to the nature of the metal used for the experiments or the temperature used.

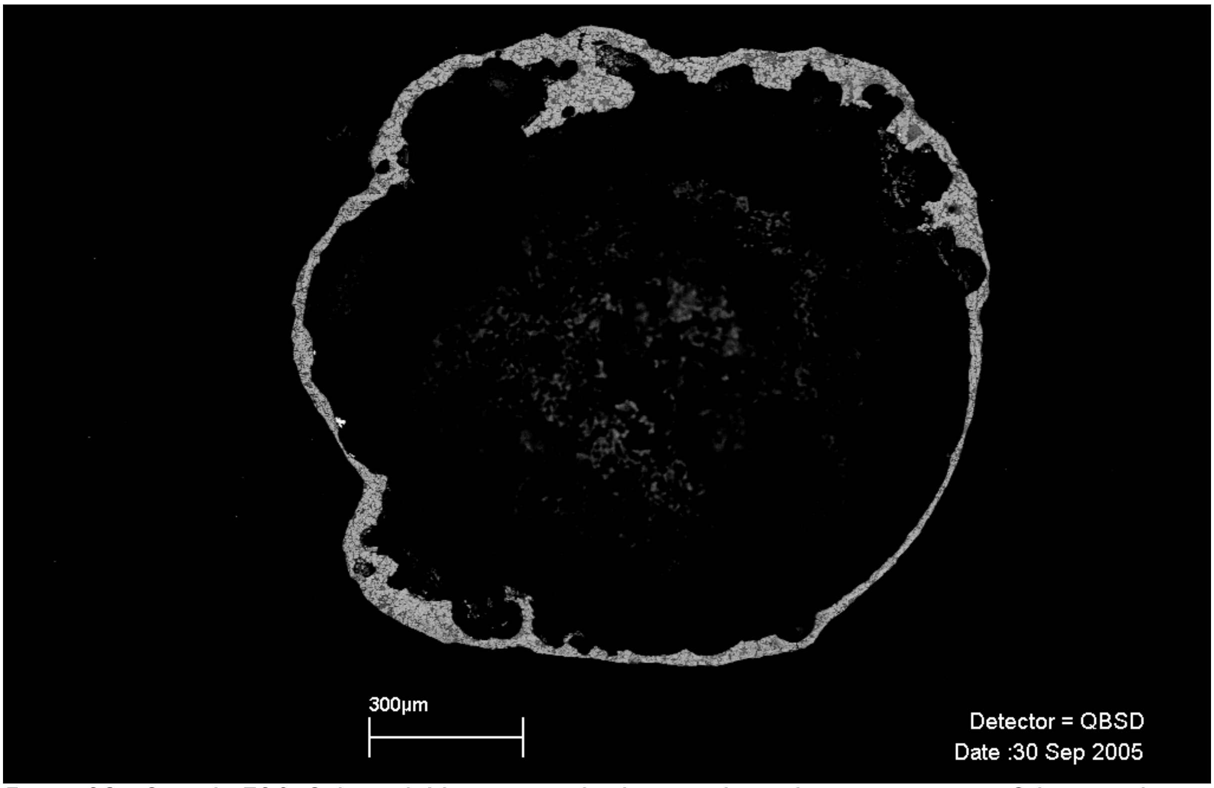

Figure 23. Sample E20. Spheroidal hammerscale showing that a large proportion of the sample is hollow

A plot of phosphorus and manganese shows that there are two compositional groups which appear to be produced from steel on the one hand and wrought iron on the other (Figure 25). This compositional difference is analogous to that seen for the flake hammerscale (Figure 20). The single exception (E18) is probably an example of contamination, ie a spheroid produced by welding steel but accidentally incorporated into the sample collected after welding iron.

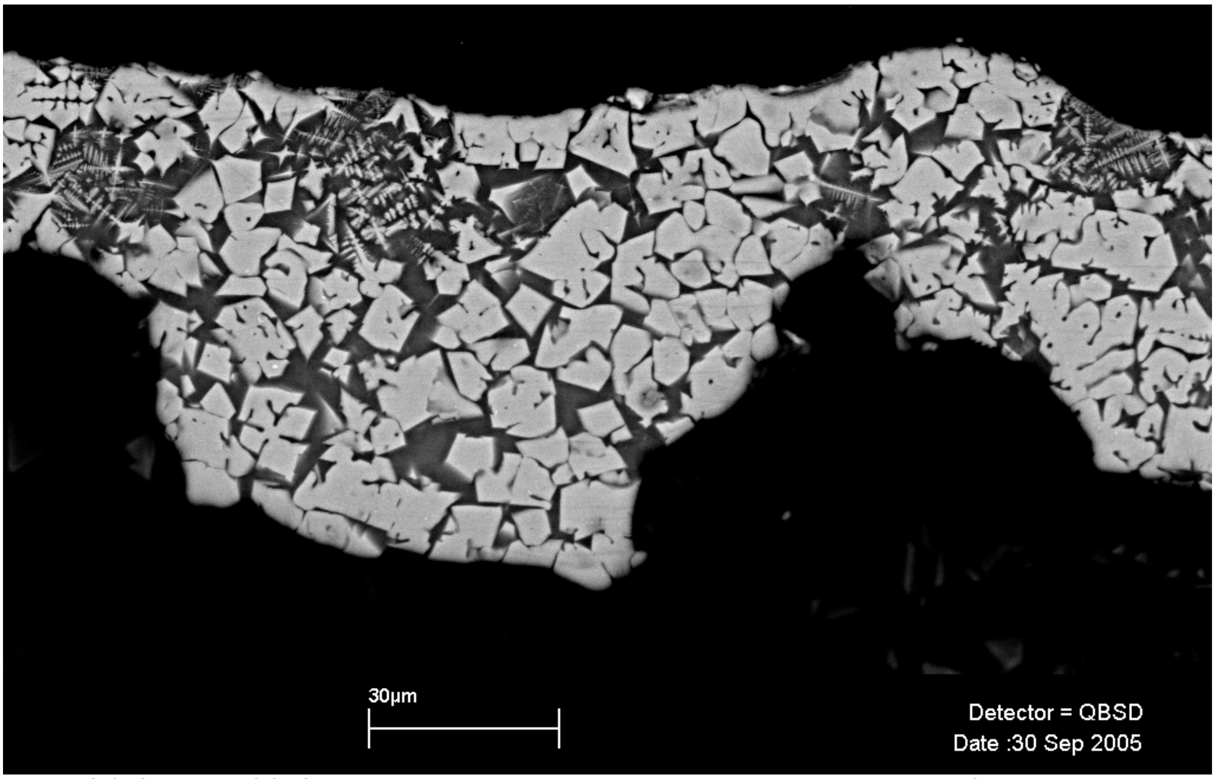

Figure 24. Sample E20. Spheroidal hammerscale showing the euhedral nature of the iron oxide (magnetite)

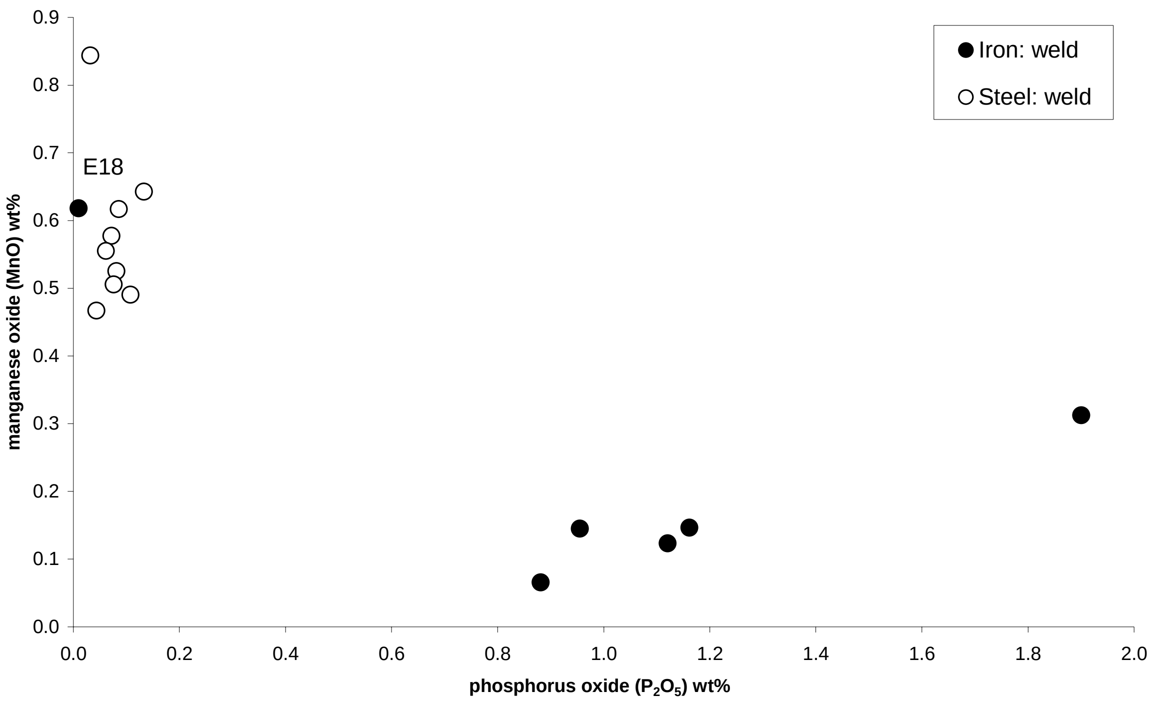

Figure 25. Manganese and phosphorus content of the spheroidal hammerscale from welding. It is likely that sample E18 is contamination

Miscellaneous hammerscale (Samples E10–15, E25–28)

Ten samples of miscellaneous hammerscale were collected during the forging and welding of wrought iron. This material makes up a small proportion of all of the hammerscale collected (7%) and was mostly associated with the working of wrought iron (Table 7). The miscellaneous hammerscale samples have a varied size and shape but many consist of half spheroids (Figure 26) or sheets with a rather bubbly texture on one surface.

Table 12. Average composition of the miscellaneous hammerscale samples (see table 8 for details of the samples). Each sample analysed 3–6 areas

	Na_2O	MgO	Al_2O_3	SiO_2	P_2O_5	SO_3	K_2O	CaO	TiO_2	MnO	Fe_3O_4
E10	0.5	0.1	1.8	6.1	0.9	4.5	<0.1	0.4	0.1	0.1	85.4
E11	0.3	0.1	1.8	9.7	2.7	3.2	0.1	0.4	0.3	0.6	80.7
E12	1.0	0.3	2.3	14.0	3.7	5.0	0.3	0.6	0.3	0.6	71.9
E13	1.0	0.3	2.9	10.9	1.7	5.5	0.2	0.6	0.2	0.3	76.5
E14	1.1	0.2	2.9	10.0	1.5	5.5	0.2	0.6	0.2	0.2	77.5
E15	1.2	0.2	2.6	8.9	1.0	3.5	0.2	0.4	0.1	0.2	81.7
E25	0.9	0.3	3.2	8.9	0.7	3.5	0.1	0.5	0.2	0.1	81.5
E26	0.4	0.1	2.4	9.4	0.8	4.3	0.2	0.4	0.1	<0.1	81.8
E27	0.2	0.2	2.4	8.1	0.7	4.2	0.2	0.4	0.2	<0.1	83.6
E28	0.5	0.2	2.4	7.3	0.7	4.0	0.1	0.4	0.2	<0.1	84.1

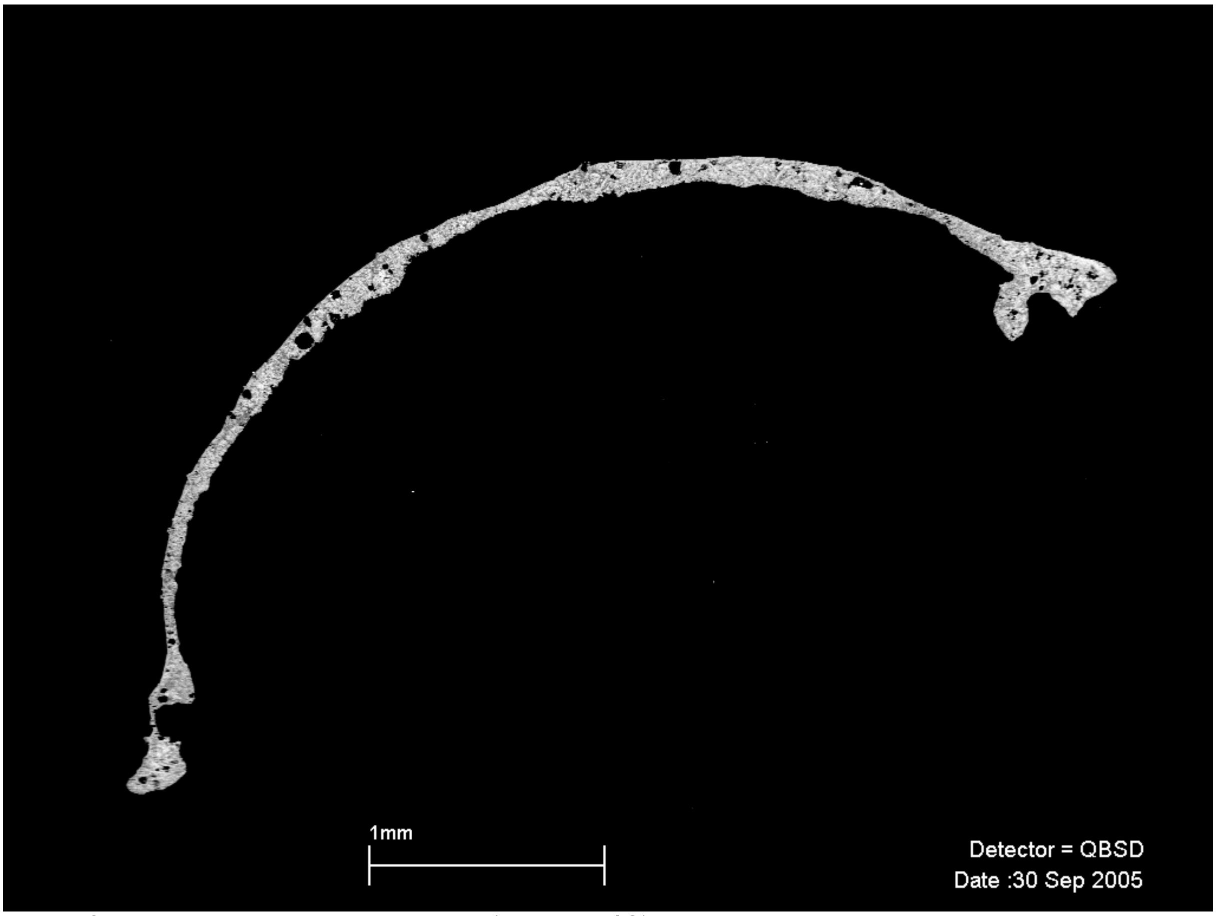

Figure 26. Miscellaneous hammerscale (sample E13)

The miscellaneous hammerscale samples show considerable variation in microstructure with euhedral equiaxed grains, laths and dendrites present in a fayalite and/or glassy matrix (Figure 27). The compositions of the miscellaneous hammerscale samples show more similarities with the spheroidal hammerscale than the flake hammerscale (Table 8).

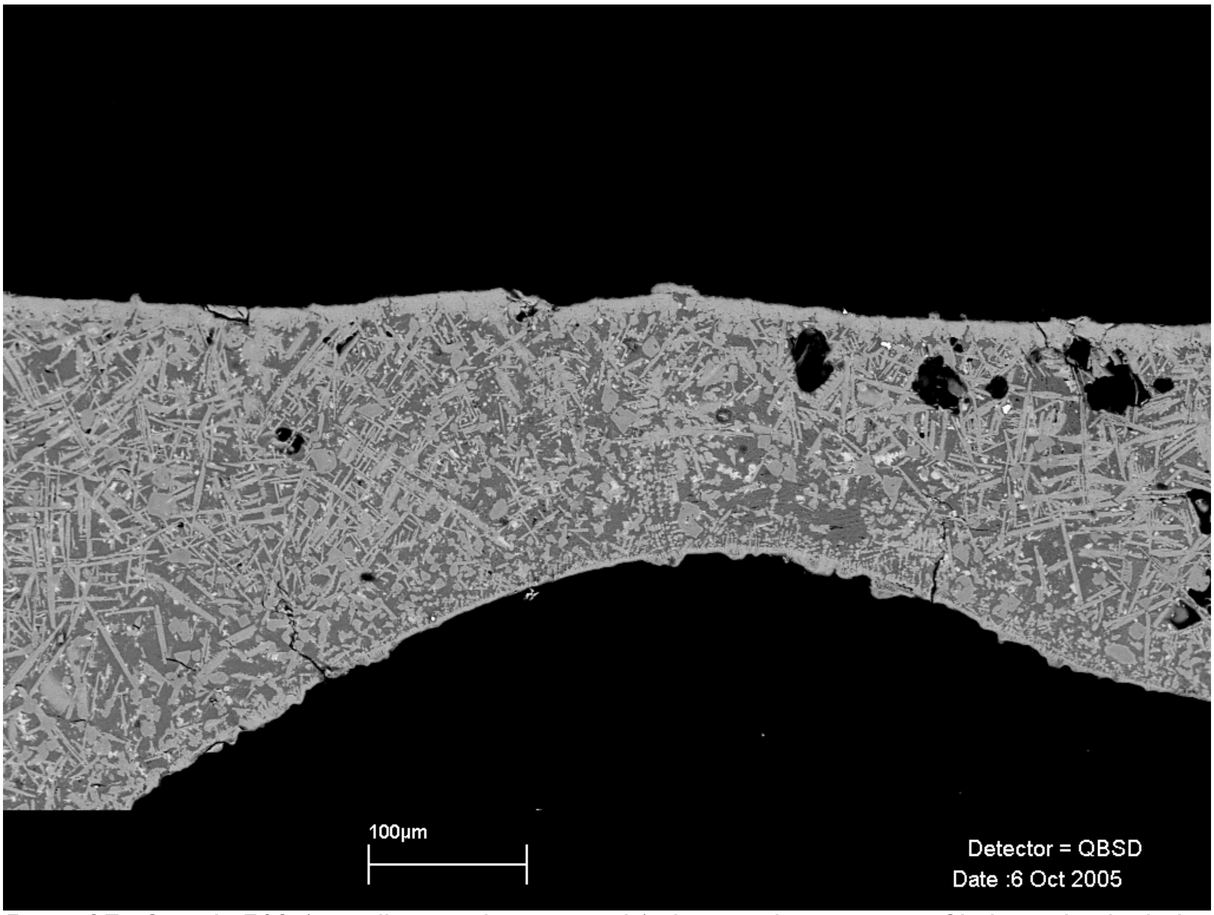

Figure 27. Sample E12 (miscellaneous hammerscale) showing the presence of laths and euhedral grains (not all phases have been identified)

Discussion of experimental hammerscale

The experimental hammerscale often displays similar results to those obtained from the archaeological material. Not all of the microstructures observed in the experimental hammerscale, however, can be found in the two groups of archaeological material. This is almost certainly due to the nature of the metal used for the experiments. The limited availability of bloomery iron meant that 19th- or 20th-century puddled wrought iron was used instead of bloomery iron. In addition, the mild steel used in the experiments would be significantly different from steel produced by the bloomery process (whether produced directly or by subsequent carburisation). The hammerscale from the experiments tends to have much higher levels of phosphorus, sulphur and manganese than the archaeological material. It is likely that these elements derive from the non-metallic inclusions in the metals used for the experiments (see below).

The spheroidal and flake hammerscale usually have distinctive microstructures. The flake hammerscale consists of large (20–100 microns) equiaxed grains (usually magnetite) in a fayalite or glassy matrix. The spheroidal hammerscale has the same phases but the magnetite is present as much smaller grains (<20 microns) with a higher proportion of fayalite or glassy matrix. The iron oxide in the experimental spheroidal hammerscale lacks the dendritic microstructure seen in the archaeological material and the reasons for this are not clear.

The flake hammerscale tends to have a high iron content while all other types have a lower iron content and increased levels of a range of other oxides. The iron oxide is negatively correlated with most of the other oxides (Figure 28) and the other oxides are also often positively correlated with each other (Figure 29).

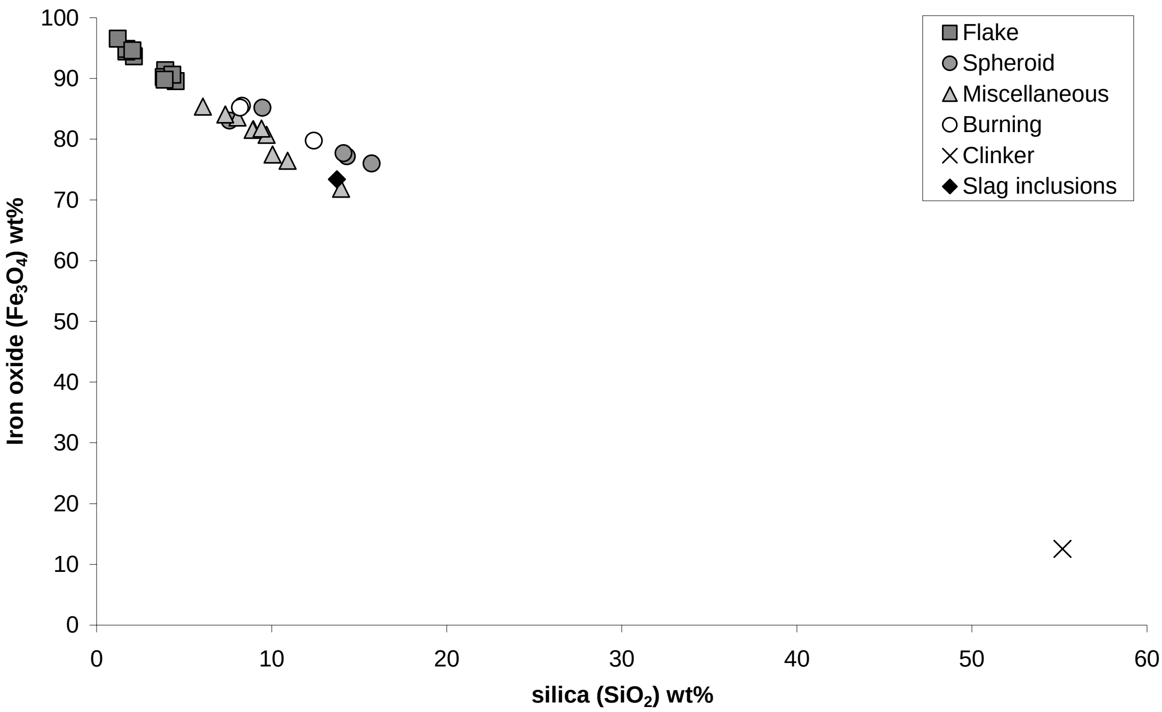

Figure 28. Silica and iron oxide contents of hammerscale from working wrought iron. The clinker and slag inclusion compositions based on chemical analyses (see Table 13)

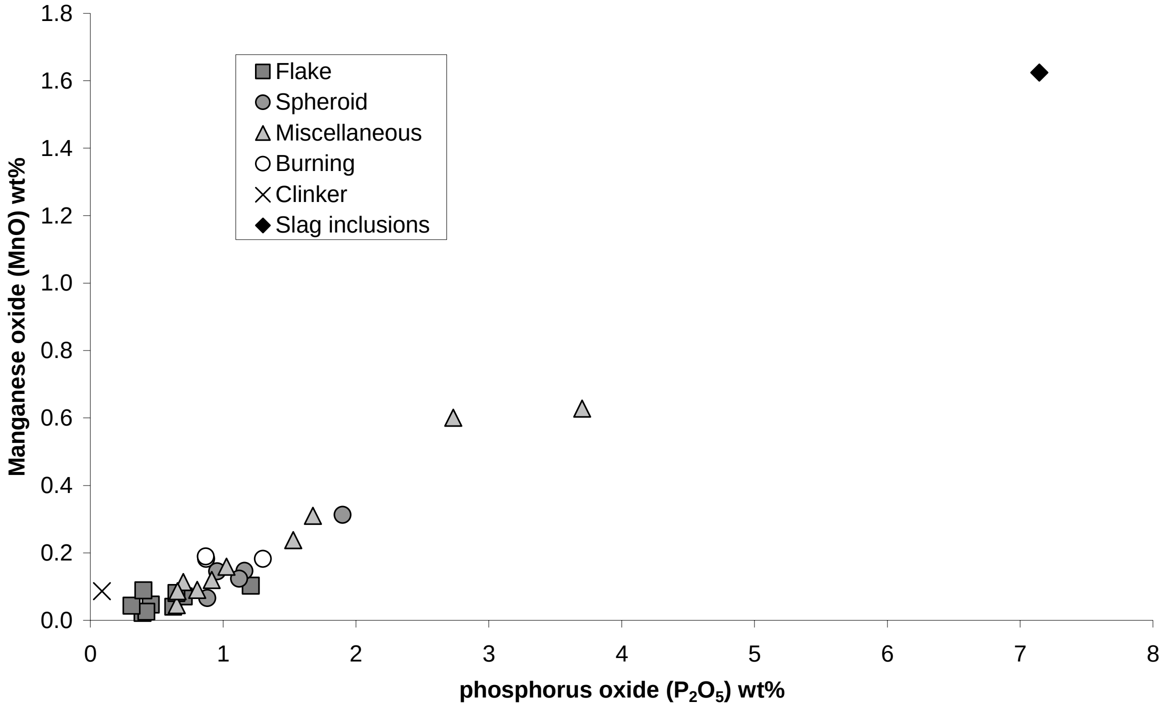

Figure 29. Phosphorus oxide and manganese oxide contents of hammerscale from working wrought iron. The clinker and slag inclusion compositions based on chemical analyses (see Table 13)

There are a number of different potential sources for the oxides other than iron but, unlike the archaeological samples, some of these can be discounted for the experimental samples. Most archaeological examples of smithing hearths were constructed with ceramic material which could theoretically have contributed a range of oxides (silica, alumina, potash, etc). The hearth used for the experiments was large and had no ceramic lining and so this source can excluded. In addition, while silica sand (or similar material) may have been used as a deliberate flux to clean the surfaces of iron from archaeological sources, no flux was used during the experiments. The two most likely sources of oxides other than iron for the experimental hammerscale are the fuel ash (referred to as clinker when present as small vitrified masses) and the non-metallic inclusions in the metal. Samples of wrought iron and clinker were prepared and analyses made of each of these two (Table 13).

Table 13. Composition of experimental hammerscale produced from wrought iron compared with the slag inclusions in the wrought iron and the clinker

	Na_2O	MgO	Al_2O_3	SiO_2	P_2O_5	SO_3	K_2O	CaO	TiO_2	MnO	Fe_3O_4
Flake	0.4	0.1	1.1	2.8	0.5	1.8	<0.1	0.1	0.1	<0.1	92.9
Spheroid	0.9	0.4	3.5	12.2	1.2	0.8	0.2	0.6	0.2	0.2	79.8
Slag inclusions	<0.1	<0.1	2.3	13.7	7.1	0.8	<0.1	0.3	0.5	1.6	73.4
Clinker	1.5	1.7	23.4	55.2	<0.1	0.1	3.0	1.1	1.3	<0.1	12.6

The plot of iron oxide and silica (Figure 28) suggests that either (or both) of these sources could have contributed to the formation of hammerscale. The plot of phosphorus and manganese (Figure 29), however, suggests that the non-metallic (slag) inclusions in the metal made the most significant contribution. The relative importance of slag inclusions is reinforced by the compositional differences between the hammerscale produced by working wrought iron and steel. That produced by working iron has low manganese and high phosphorus contents, while that produced by working steel has the reverse (Figures 20 and

25). This appears to be a reflection of the differences in the composition of the non-metallic inclusions in the metals used. The wrought iron contains slag inclusions which have relatively high levels of phosphorus and low levels of manganese (Table 13), while the mild steel contains inclusions that are rich in manganese and have low levels of phosphorus. Unfortunately, no sample of the mild steel used in experiments was retained; the later collection of several samples of stock mild steel from West Dean showed a variety of non-metallic inclusions present , including manganese sulphides, manganese silicates and aluminium-calcium-silicates.

A model for the formation of hammerscale

Flake hammerscale

The oxidation of iron is a topic of considerable interest in contemporary steel fabrication (due to the potential loss of material) and the formation of scale has been thoroughly studied (eg Birk and Meier 1983; Birosca *et al* 2004; Chen and Yeun 2003; Garber 1959; Iordanova *et al* 2000; Kubaschewski and Hopkins 1962). Experimental studies reviewed by Chen and Yeun (2003, 435–7) indicate that initial growth is fast but that the rate of growth slows as the oxide layer becomes thicker (see Figure 30). Experimental work has also shown that the thickness of the oxide layer (for a given time) increases with temperature (Figure 31). The growth of oxide layers is affected by the nature of the metal: carbon-free iron tends to oxidise more quickly that iron-carbon alloys (including steels). The situation with modern alloy steels is complex, depending on whether the alloying elements are more or less easily oxidised than iron, however, these alloys are of limited relevance to archaeological material.

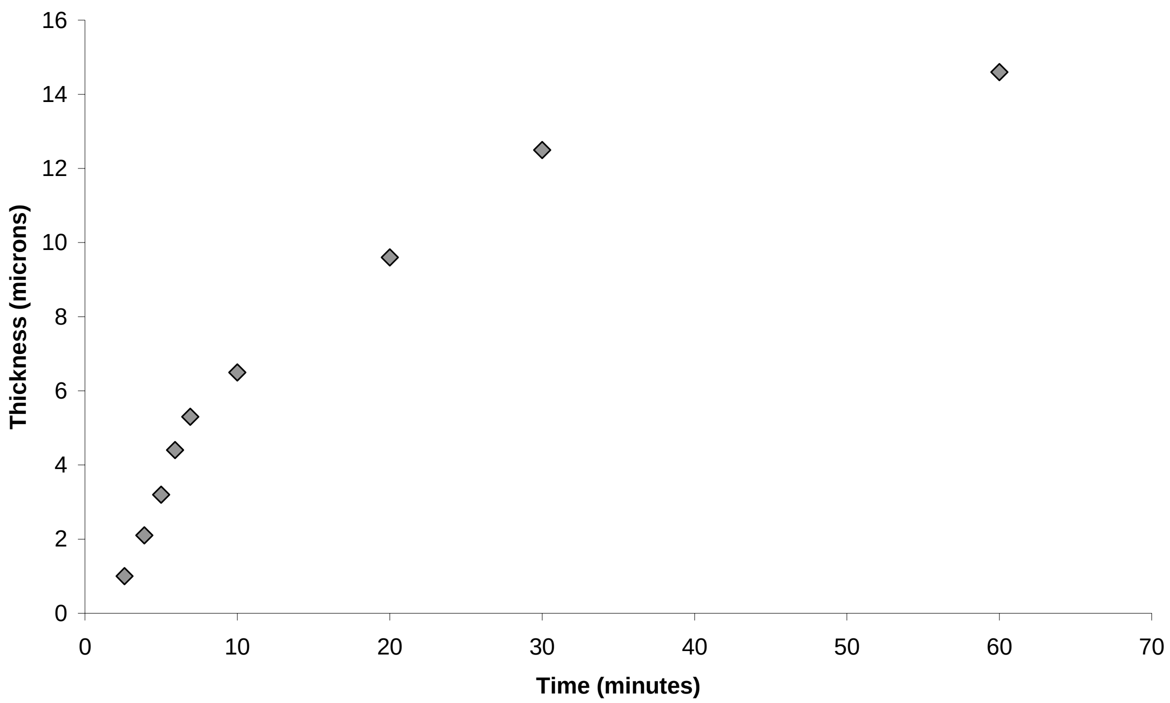

Figure 30. The thickness of oxide layer formed on low carbon steel at 600ºC (after Iordanova et al *2000, figure 3)*

The nature of the oxide surface that forms on iron depends primarily on the temperature. Below 570°C, the oxide surface contains two layers, an inner layer of magnetite (Fe_3O_4) and an outer layer of hematite (Fe_2O_3), above 570°C the oxide surface contains three layers, a thick inner layer of wüstite (FeO), a thin intermediate layer of magnetite, and an extremely thin outer layer of hematite. The wüstite layer is the thickest as the 'diffusion coefficient of iron in wüstite is much greater than in magnetite and the diffusion of oxygen and iron through the hematite layer is extremely slow' (Chen and Yuen 2003, 435). While the wüstite layer is thickest during high-temperature oxidation, it is not thermodynamically stable below 570°C and 'magnetite precipitation within the wüstite layer is essentially inevitable' (Chen and Yuen 2003, 436). Magnetite precipitation depends primarily on cooling rate but appears to be extensive in both the archaeological and experimental samples examined here.

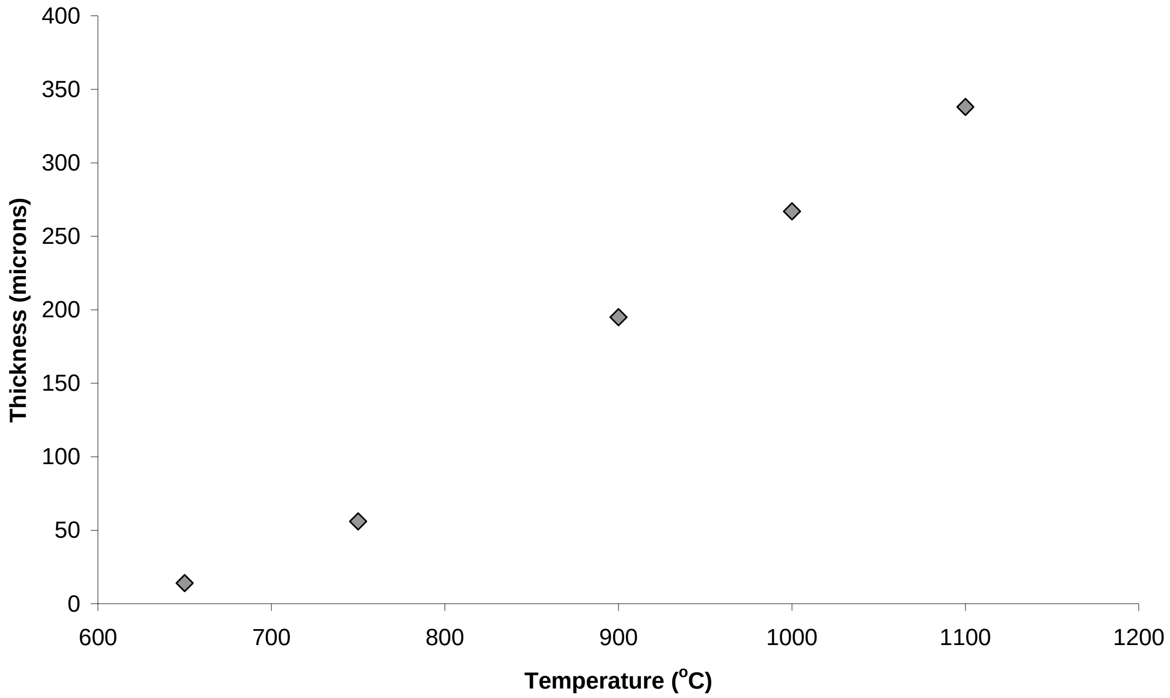

Figure 31. The thickness of oxide layer formed on carbon-free iron after 60 minutes (after Birosca et al *2004)*

The chemical composition of the archaeological and experimental flake hammerscale varies a little. Its iron oxide content varies from slightly less than 90wt% to just over 95wt% with the balance being made up of silica, alumina, and the oxides of sulphur, phosphorus and manganese. The compositional differences between the flakes produced from steel and those from wrought iron are striking (Figure 20). This suggests that the non-iron content of flake hammerscale derives primarily from the non-metallic inclusions in the metal.

The thickness of the flake hammerscale will depend on the heating temperature and the duration of the heating. Blacksmiths traditionally judged the correct temperature for forging (and welding) iron and steel from the colour of the metal, however advice on judging colour was often conflicting. The CSIRA (1952, 19) recommends judging the colour of heated iron in daylight while Bealer (1995, 124) recommends judging colour in a darkened environment, such as a barrel or box. The hotworking of iron usually relies on heating iron to a sufficiently high temperature (>910°C) to allow the transformation of ferrite into austenite. However, temperatures much higher than this were usually avoided as they accelerate oxidation and can even lead to combustion. Higher temperatures would have been employed when welding, between 1100° and 1300°C. Modern high-temperature working of steel often makes use of large billets and so requires long heating times, however, most archaeological iron objects are much smaller and so would have required relatively short heating times. It is unlikely that blacksmiths would have heated small pieces of iron for longer than 10 minutes. Assuming a heating temperature of 1000°C and a heating time of 5 minutes, the thickness of scale produced on carbon-free iron would be approximately 50 microns (cf Birosca *et al* 2004, fig 2). Most archaeological examples of flake hammerscale are substantially thicker than 50 microns but often display a series of distinct layers some of which are roughly 50 microns thick (cf Figure 3). It is proposed that flake hammerscale often grew *in situ* through several heats. When considering the growth of flake hammerscale during heating prior to fire-welding, the higher temperature and longer duration of the heating will produce thicker layers of flake hammerscale. Assuming a heat of 1200°C and duration of 10 minutes, the thickness of the scale produced on carbon-free iron would be approximately 300 microns (cf Birosca *et al* 2004, Fig 2).

Spheroidal hammerscale

The experimental forging and fire-welding of wrought iron and mild steel has shown that spheroidal material is produced during fire-welding and during the combustion of these metals. While the combustion of ferrous alloys is of considerable interest in modern industries there appears (unsurprisingly) to be no scientific literature on fire-welding. The limited literature on the combustion of iron usually focuses on oxygen-rich environments (Bolobov 2001; Charles and Chater 1978; Sato *et al* 1995; Steinberg *et al* 1992) which may not be entirely applicable to a blacksmith's hearth.

As iron is heated in an atmosphere containing oxygen, an oxide layer grows at the surface as described above. This oxide layer provides a degree of protection for the underlying metal but only while the oxide remains as a solid. Once the oxide surface melts, it ceases to provide any protection and the metal will oxidise very rapidly — it combusts. The bulk of the oxide surface on iron is made up of wüstite which melts at 1371°C (the other oxides form a small proportion of the surface layer and have higher melting temperatures) but experimental work by Bolobov (2001) and Sato *et al* (1995) has shown that combustion of iron and mild steel occurs from1250°C. Unfortunately the iron combustion literature contains little observation on the form of the material resulting from combustion. As the burnt material moves away from the metal it will be in a liquid state and consist entirely of oxides (or have an outer surface of oxides) and so will have a high surface tension. Therefore it is likely that the material will form spheroids which due to the high surface area will cool quickly and so should retain this shape.

The oxygen cutting of iron (Charles and Chater 1978) relies on preheating the metal and then introducing a stream of oxygen. The heated iron reacts with the oxygen generating more heat, leading to a limited form of combustion which cuts through the metal. Charles and Chater observed that the slag collected from the bottom of their experimental cuts 'are always in the form of hollow droplets when cold' (ibid, 166) and suggest that the hollow form is due to the liberation of gas during cooling but before the outer surface solidifies. A similar mechanism may explain the formation of hollow spheroids during fire-welding. In particular the ejection of metal oxides and slag from the weld line will lead to a drop in temperature and pressure which may lead to the liberation of gas.

Conclusions and recommendations

The SEM images of flake hammerscale have shown that they usually have relatively large equiaxed iron oxide grains with a small amount of silicate material along grain boundaries. The archaeological flake hammerscale is comparable to the experimentally produced material, and to scale surfaces observed on modern iron subject to heating in air. It is likely that a single period of heating for ordinary forging would produce an oxide layer 50 microns thick, while heating prior to welding would produce a layer 300 microns thick. Some archaeological samples of flake hammerscale display a series of layers which may indicate more than one period of heating before the flake became detached. The examination of the experimental flake hammerscale showed no significant differences in thickness between that collected from forging experiments and that collected from welding experiments.

The spheroidal hammerscale from archaeological contexts has a more variable microstructure than the flakes but most commonly this consists of a hollow spheroid, the skin of which contains fine iron oxide dendrites in a silicate matrix. Unlike the flake hammerscale, spheroidal hammerscale has clearly been molten at some stage. The experimentally produced spheroidal hammerscale rarely had a microstructure comparable with the archaeological specimens, possibly due to the nature of the experiment and the materials used.

An examination of the chemical composition of the various types of hammerscale suggests that non-metallic inclusions in the parent iron or iron alloy make a significant contribution, especially to the spheroidal material; the non-metallic inclusions in iron and steel act as a flux. The compositions of the archaeological samples provides no evidence for the use of a separate flux (and the experimental welding was achieved without the use of a flux).

The collection of hammerscale produced at each stage of the experiments shows that spheroidal hammerscale is mainly associated with fire-welding. The high-speed digital video confirms that spheroids are produced by welding, and that they emerge from the weld line as an amorphous stream of material which coalesces into a series of spheroids within 0.03 seconds. Subsequent examination of samples suggests that there was a degree of contamination in later samples due to the failure to completely clean the floor after each stage.

The deliberate burning of iron and steel was relatively easily achieved and showed that spheroidal material could be produced by this process. In the case of the mild steel, the burnt spheroids had a distinctive microstructure different from that of the welding spheroids. The situation with wrought iron is less clear.

Further work can be recommended to address some of the issues which this project was not able to fully answer; primarily the failure to produce experimental spheroids with microstructures comparable to the archaeological examples. The experiments to fire-weld iron should be undertaken by a more experienced smith, using bloomery iron, a clay-built hearth and charcoal fuel. The problems of contamination between each stage could be addressed either through the use of a vacuum cleaner or by restricting the experiment to a single metal and process.

Acknowledgements

We would like to thank Vincent Guichard and all the staff and colleagues at the Centre Archéologique Européen de Mont Beuvray, Glux en Glenne, Saône et Loire, France who provided access to Mont Beuvray for the archaeological teams from English Heritage and the University of Southampton. The excavation of the first-century BC blacksmiths workshops allowed the collection of large quantities of hammerscale. We are grateful to Howard Brooks of Colchester Archaeological Trust who provided the samples of hammerscale from 79 Hythe Hill, Colchester. We would like to thank Tonny Bentjes and West Dean College who provided access to the blacksmithing workshops (and lunch!). Andrew Breese (one time tutor on the blacksmithing courses) provided initial guidance on how to forge and weld iron and steel, and continued to supervise the experimental stages. Eleanor Blakelock and Vanessa Fell provided assistance during the experimental forging and welding at West Dean. Much of the interpretation has emerged through discussions with colleagues, in particular Ted Steinberg, Vincent Serneels, Tim Young, Chris Salter and Jim Charles.

References

Allen, J R L 1986 'Interpretation of some Romano-British smithing slag from Awre in Gloucestershire'. *Historical Metallurgy* **20**, 97–104

Bayley, J, Dungworth, D and Paynter, S 2001 *Archaeometallurgy*. English Heritage Guidelines. London: English Heritage

Bealer, A 1995 *The Art of Blacksmithing*. Edison, NJ: Castle

Birk, N and Meier, G H 1983 *Introduction to High Temperature Oxidation of Metals*. London: Edward Arnold

Birosca, S, Dingley, D and Higginson, R L 2004 'Microstructural and microtextural characterization of oxide scale on steel using electron backscatter diffraction'. *Journal of Microscopy* **213**, 235–40

Bolobov, V I 2001 'Conditions for ignition of iron and carbon steel in oxygen'. *Combustion, Explosion, and Shock Waves* **37**, 292–296

Brooks, H 2000 'Excavations at 79 Hythe Hill, Colchester 1994–5'. *Essex Archaeology and History* **31**, 112–124

Charles, J A and Chater, W J B 1978 'Oxygen cutting'. *Metals Technology* **5**, 163–175

Chen, R Y and Yeun, W Y D 2003 'Review of the high-temperature oxidation of iron and carbon steels in air or oxygen'. *Oxidation of Metals* **59**, 433–68

CSIRA 1952 *The Blacksmith's Craft*. Salisbury: the Council for Small Industries in Rural Areas

Dungworth, D forthcoming 'Examination of metalworking debris from the 1939 excavations at Trevelgue Head', *in* Nowakowski, J and Quinnell, H *Trevelgue Head, Cornwall – an Iron Age cliff-castle: the story of the 1939 excavations by the late C K Croft Andrew*. Truro: Cornwall County Council

Forster, R H and Knowles, W H 1910 'Corstoptium: report on the excavations in 1909'. *Archaeologia Aeliana* **6**, 205–272

Forster, R H and Knowles, W H 1913 'Corstoptium: report on the excavations in 1912'. *Archaeologia Aeliana* **9**, 230–280

Garber, S 1959 'Fundamental aspects of scale on mild-steel strip'. *Journal of the Iron and Steel Institute* **192**, 153–160

Guichard, V, Barral, P, Beck, P, Bonenfant, P-P, Boyer, F, Creighton, J, Dhennequin, L, Dominguez-Arranz, A, Dufay-Flouest, A, Dungworth, D, Durost, S, Gran-Aymerich, J, Gruel, K, Guillaumet, J-P, Hamm, G, Haselgrove, C, Jouffroy-Bapicot, I, Lambert, G, Laszlovsky, J, Lowther, P, Luginbühl, T, Monna, F, Olmer, F, Paris, P, Paunier, D, Petit, C, Popovitch, L, Richard, H, Rieckhoff, S, Schubert, F, Szabó, M, Toledo I Mur, A, Urban, O, Vitali, D and Wiethold, J 2003 'Un aperçu des acquis récents des recherches sur l'oppidum de Bibracte (1997–2002)'. *Revue d'Archéologique de l'Est* **52**: 45–90

Iordanova, I, Surtchev, M, Forcey, K S and Krastev, V 2000 'High-temperature surface oxidation of low-carbon rimming steel'. *Surface and Interface Analysis* **30**, 158–160

Jackson, C, Booth, C A and Smedley, J W 2005 'Glass by design? Raw materials, recipes and compositional data'. *Archaeometry* **47**, 781–795

Kofstad, P 1966 *High Temperature Oxidation of Metals*. Chichester: Wiley

Kubaschewski, O and Hopkins, B E 1962 *Oxidation of Metals and Alloys*. London: Butterworths

McDonnell, G 1984 'The study of early iron smithing residues', *in* Scott, B G and Cleere, H (eds) *Crafts of the Blacksmith*. Belfast UISPP, 47–52

McDonnell, G 1986 *The Classification Of Early Iron Working Slags*. Unpublished PhD thesis, University of Aston, Birmingham

McDonnell, G 1991 'A model for the formation of smithing slags'. *Materialy Archeologiczne* **26**, 23–28

Mills, A and McDonnell, G 1992 *The identification and analysis of the hammerscale from Burton Dassett Warwickshire*. Ancient Monuments Laboratory report 47/1992. London: English Heritage

Paynter, S 2002 *The metalworking remains from Westhawk Farm, near Ashford, Kent.* Centre for Archaeology report 84/2002. London: English Heritage

Paynter, S 2006 'Regional variations in bloomery smelting slag of the Iron Age and Romano-British periods'. *Archaeometry* **48**, 271–292

Richmond, I A and Birley, E 1940 'Excavations at Corbridge'. *Archaeologia Aeliana* **17**, 85–115

Sato, J, Ohtani, H, and Hirano, T 1995 'Ignition process of a heated iron block in high-pressure oxygen atmosphere'. *Combustion and Flame* **100**, 376–383

Sim, D 1998 *Beyond the Bloom*. BAR International Series 725. Oxford: British Archaeological Reports

Simpson, FG and Richmond, I A 1941 'The Roman Fort on Hadrian's Wall At Benwell'. *Archaeologia Aeliana* **19** , 1–43

Starley, D 1997 *The analysis of slag and other metalworking debris from Creeton Quarry, Lincs.* AML Report 99/1997. London: English Heritage

Starley, D 2000 'Metalworking debris', in Buxton, K and Howard-Davis, C *Bremetenacum; excavations at Roman Ribchester 1980, 1989–1990*. Lancaster: University of Lancaster Archaeology Unit, 337–47

Steinberg, T A, Mulholland, G P, Wilson, B and Benz, F J 1992 'The combustion of iron in high-pressure oxygen'. *Combustion and Flame* **89**, 221–228

Turner, W E S 1956 'Studies in ancient glasses and glassmaking processes. Part V. Raw materials and melting processes'. *Journal of the Society of Glass Technology* **40**, 277T–300T

Tylecote, R F and Owles, E 1960 'A second-century iron smelting site at Ashwicken, Norfolk'. *Norfolk Archaeology* **32**, 142–162

Tylecote, RF 1962 *Metallurgy in Archaeology*. London: Edward Arnold

Unglik, H 1991 'Observations on microscopic smithing residues from Bixby Blacksmith Shop, Barre Four Corners, USA 1824–55'. *Historical Metallurgy* **25**, 92–98